

Supporting Information

Isonitrile induced bioorthogonal activation of fluorophores and mutually orthogonal cleavage in live cells

Xiaoyang Zhang,^a Hui Xu,^b Jie Li,^b Dunyan Su,^b Wuyu Mao,^b Guohua Shen,^a Lin Li ^a
and Haoxing Wu ^{*b}

^a Laboratory of Clinical Nuclear Medicine, Department of Nuclear Medicine, West China Hospital, Sichuan University, Chengdu, 610041, China

^b Huaxi MR Research Center, Department of Radiology, Functional and Molecular Imaging Key Laboratory of Sichuan Province, National Clinical Research Center for Geriatrics, West China Hospital, Sichuan University, Chengdu, 610041, China

* To whom correspondence should be addressed: haoxingwu@scu.edu.cn

Table of contents

1. General considerations	S3
2. Synthesis	S4
3. Absorption and fluorescence emission spectra of <i>t</i>BuTz-caged probes before and after cleavage reaction	S13
4. Fluorescence quenching efficiency of vinyl ether in the literature	S17
5. The stability and activation of quenched probes in buffer and cell culture medium	S18
6. Fluorophore release monitored by LC-MS	S20
7. Preparation and characterization of oligonucleotide probes	S23
8. Fluorescence turn-on via DNA templated cleavage	S28
9. Fluorescence turn-on via RNA templated cleavage	S29
10. The stability and activation of <i>i</i>PrTz-DAO	S30
11. Mutually orthogonal release of fluorophores involving DNA template	S31
12. Mutually orthogonal release of fluorophores involving RNA template	S32
13. Live cell confocal fluorescence imaging	S33
14. Spectra (¹H NMR, ¹³C NMR, HRMS)	S35

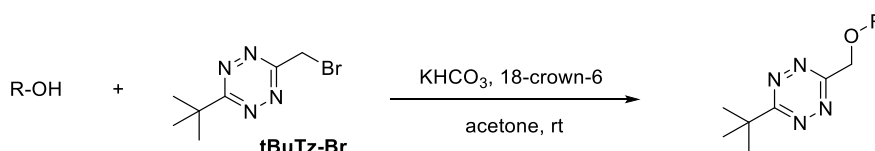
1. General considerations

All chemical reagents were purchased from commercial sources (eg. J&K Scientific, TCI, Energy Chemical, and Bide Pharm) and used as received. All oligonucleotides were purchased from Sangon Biotech. Thin layer chromatography (TLC) was performed on silica gel plates (glass back, Yantai Jiangyou Silica gel Development Co., LTD) and visualized under ultraviolet (UV) light (254 nm, 365 nm). Normal phase silica gel chromatography was conducted on silica gel from Titan Scientific (200-300 mesh). ^1H (400 MHz) and ^{13}C (101 MHz) NMR spectra were acquired on a Bruker AV400 instrument. Chemical shifts (δ) were reported in ppm, and the ^{13}C NMR were proton decoupled. LC-MS spectrometry was performed on an Agilent 1260 Infinity HPLC system equipped with a G6125B Single Quadrupole MS system. High-resolution mass spectra (HRMS) were obtained on a Bruker micro-TOF-QII mass spectrometer (electrospray ionization). UV-Vis absorption spectra were collected on a Quawell Scientific Q6000+ micro volume spectrophotometer, oligonucleotide concentrations were measured by the absorbance at 260 nm. Fluorescence measurements were conducted on a FluoroMax-4 fluorometer (Jobin Yvon, Horiba) or a TECAN Spark multifunctional microplate reader. Live cell confocal fluorescence imaging was conducted on a LSM 880 system (Carl ZEISS). All mixed solvents are expressed as volume ratio.

2. Synthesis

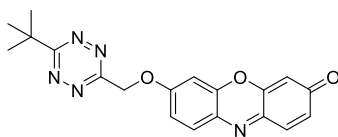
Known compounds were synthesized according to the literature: 3-(bromomethyl)-6-(*tert*-butyl)-1,2,4,5-tetrazine (**tBuTz-Br**, *Chem. Sci.*, 2020, **11**, 169-179), FL-OH (*J. Am. Chem. Soc.*, 2016, **138**, 11429-11432), DHX-OH (*ACS Appl. Mater. Interfaces*, 2017, **9**, 6796-6803), DAO-OH (*Angew. Chem. Int. Ed.*, 1991, **103**, 1646-1648), methyl 4-isocyanobutanoate (**3a**, *Green Chem.*, 2020, **22**, 6902-6911).

General synthesis procedure for *t*BuTz quenched fluorogenic probes



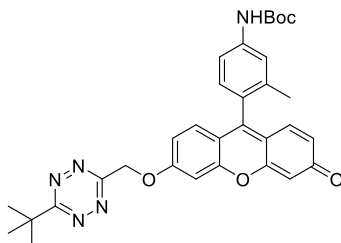
R-OH (0.10 mmol), KHCO_3 (30.0 mg, 0.30 mmol), 18-crown-6 (6.6 mg, 0.025 mmol), and acetone (1.0 mL) were added into a round bottom flask (5 mL) equipped with a magnetic stir bar. Cooled and stirred in an ice bath, the mixture was added dropwise with **tBuTz-Br** (27.6 mg, 0.12 mmol, dissolved in 0.2 mL acetone). The reaction mixture was brought to room temperature and stirred overnight. Purification by TLC plate afforded the product.

7-((6-(*tert*-butyl)-1,2,4,5-tetrazin-3-yl)methoxy)-3*H*-phenoxazin-3-one (**1a**, **tBuTz-RSF**)



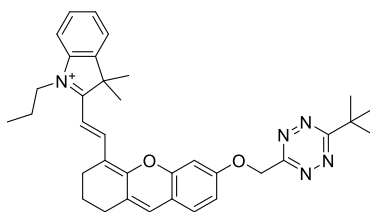
Yield, 30.6%. ^1H NMR (400 MHz, Chloroform-*d*) δ 7.75 (d, $J = 8.9$ Hz, 1H), 7.42 (d, $J = 9.8$ Hz, 1H), 7.11 (dd, $J = 8.8, 2.6$ Hz, 1H), 7.03 (d, $J = 2.6$ Hz, 1H), 6.84 (dd, $J = 9.8, 1.8$ Hz, 1H), 6.33 (d, $J = 1.8$ Hz, 1H), 5.76 (s, 2H), 1.62 (s, 9H). ^{13}C NMR (101 MHz, CDCl_3) δ 186.28, 177.29, 164.30, 161.57, 149.62, 146.35, 145.48, 134.73, 134.49, 131.81, 128.98, 113.84, 106.94, 101.50, 68.25, 38.32, 29.15. HRMS $[\text{M}+\text{H}]^+$ m/z calcd. for $[\text{C}_{19}\text{H}_{18}\text{N}_5\text{O}_3]^+$ 364.1404, found 364.1403.

tert-butyl (4-(6-((6-(tert-butyl)-1,2,4,5-tetrazin-3-yl)methoxy)-3-oxo-3H-xanthen-9-yl)-3-methylphenyl)carbamate (1b, tBuTz-FL)



Yield, 49.4%. ^1H NMR (400 MHz, Chloroform-*d*) δ 7.50 (s, 1H), 7.33 (dd, $J = 8.3, 1.9$ Hz, 1H), 7.14 (d, $J = 2.4$ Hz, 1H), 7.08 (d, $J = 8.2$ Hz, 1H), 7.06 (d, $J = 8.9$ Hz, 1H), 6.99 (d, $J = 9.7$ Hz, 1H), 6.92 (dd, $J = 8.9, 2.5$ Hz, 1H), 6.64 (s, 1H), 6.57 (dd, $J = 9.7, 1.8$ Hz, 1H), 6.45 (d, $J = 1.8$ Hz, 1H), 5.76 (s, 2H), 2.05 (s, 3H), 1.61 (s, 9H), 1.56 (s, 9H). ^{13}C NMR (101 MHz, CDCl_3) δ 185.88, 177.27, 164.34, 162.34, 158.88, 154.41, 152.80, 149.18, 139.80, 137.32, 130.75, 130.24, 129.88, 126.59, 120.15, 119.11, 116.11, 115.54, 113.62, 105.90, 101.66, 81.01, 68.08, 38.31, 29.15, 28.35, 19.92. HRMS $[\text{M}+\text{H}]^+$ m/z calcd. for $[\text{C}_{32}\text{H}_{34}\text{N}_5\text{O}_5]^+$ 568.2554, found 568.2557.

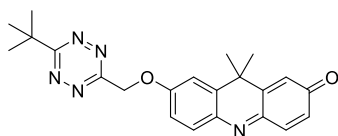
(E)-2-(2-(6-((6-(tert-butyl)-1,2,4,5-tetrazin-3-yl)methoxy)-2,3-dihydro-1H-xanthen-4-yl)vinyl)-3,3-dimethyl-1-propyl-3H-indol-1-ium (1c, tBuTz-DHX)



Yield, 32.3%. ^1H NMR (400 MHz, Methanol-*d*₄) δ 8.80 (d, $J = 14.9$ Hz, 1H), 7.66 (d, $J = 7.3$ Hz, 1H), 7.61 – 7.42 (m, 4H), 7.38 (s, 1H), 7.29 (d, $J = 2.2$ Hz, 1H), 7.14 (dd, $J = 8.6, 2.4$ Hz, 1H), 6.56 (d, $J = 14.9$ Hz, 1H), 5.86 (s, 2H), 4.35 (t, $J = 7.4$ Hz, 2H), 2.79 (t, $J = 6.0$ Hz, 2H), 2.73 (t, $J = 6.1$ Hz, 2H), 2.02 – 1.90 (m, 4H), 1.85 (s, 6H), 1.59 (s, 9H), 1.08 (t, $J = 7.4$ Hz, 3H). HRMS $[\text{M}+\text{H}]^+$ m/z calcd. for $[\text{C}_{35}\text{H}_{40}\text{N}_5\text{O}_2]^+$ 562.3177, found 562.3174.

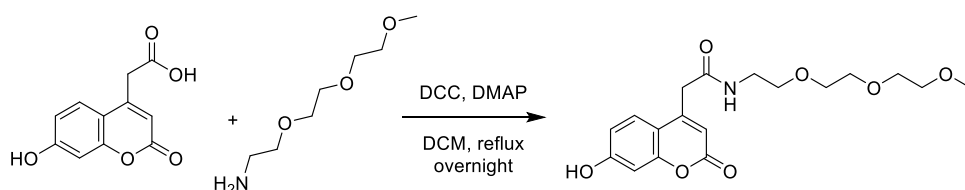
7-((6-(tert-butyl)-1,2,4,5-tetrazin-3-yl)methoxy)-9,9-dimethylacridin-2(9H)-one (1d,

***t*BuTz-DAO)**



Yield, 25.4%. ¹H NMR (400 MHz, Chloroform-*d*) δ 7.67 (d, *J* = 8.7 Hz, 1H), 7.39 (d, *J* = 9.7 Hz, 1H), 7.21 (d, *J* = 2.7 Hz, 1H), 7.08 (dd, *J* = 8.7, 2.8 Hz, 1H), 6.69 – 6.60 (m, 2H), 5.74 (s, 2H), 1.61 (s, 9H), 1.53 (s, 6H). ¹³C NMR (101 MHz, CDCl₃) δ 187.16, 177.18, 164.72, 160.01, 151.14, 147.41, 141.70, 139.75, 137.50, 133.81, 131.38, 127.59, 113.51, 113.10, 67.99, 38.29, 37.40, 32.41, 29.16. HRMS [M+H]⁺ *m/z* calcd. for [C₂₂H₂₄N₅O₂]⁺ 390.1925, found 390.1920.

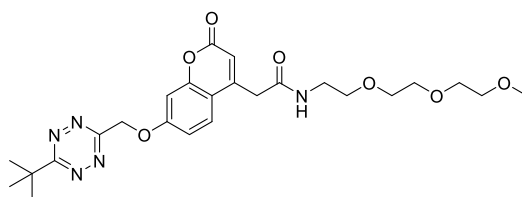
2-(7-hydroxy-2-oxo-2H-chromen-4-yl)-N-(2-(2-(2-methoxyethoxy)ethoxy)ethyl)acetamide (CM-OH)



To a mixture of 7-hydroxycoumarinyl-4-acetic acid (1.60 g, 7.2 mmol), DCC (1.48 g, 7.2 mmol) and DMAP (72 mg, 0.6 mmol) in DCM was added 2-(2-(2-methoxyethoxy)ethoxy) ethanamine (960 mg, 6.0 mmol). The resulting mixture was stirred at 40 °C overnight, then evaporated under reduced pressure. The residue was purified on silica column chromatography to afford the desired product in 79% yield.

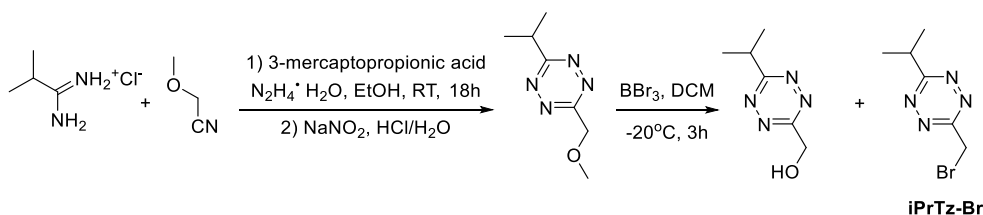
¹H NMR (400 MHz, DMSO-*d*₆) δ 10.53 (s, 1H), 8.29 (t, *J* = 5.5 Hz, 1H), 7.60 (d, *J* = 8.7 Hz, 1H), 6.78 (dd, *J* = 8.7, 2.3 Hz, 1H), 6.71 (d, *J* = 2.3 Hz, 1H), 6.16 (s, 1H), 3.65 (s, 2H), 3.56 – 3.46 (m, 6H), 3.45 – 3.38 (m, 4H), 3.28 – 3.17 (m, 5H). ¹³C NMR (101 MHz, DMSO-*d*₆) δ 168.22, 161.62, 160.70, 155.47, 151.74, 127.16, 113.33, 112.11, 111.96, 102.75, 71.74, 70.19, 70.08, 70.06, 69.41, 58.52, 39.35, 39.24. HRMS [M+Na]⁺ *m/z* calcd. for [C₁₈H₂₃NNaO₇]⁺ 388.1367, found 388.1369.

*2-(7-(((6-(tert-butyl)-1,2,4,5-tetrazin-3-yl)methoxy)-2-oxo-2H-chromen-4-yl)-N-(2-(2-(2-methoxyethoxy)ethoxy)ethyl)acetamide (1e, *t*BuTz-CM)*



Yield, 53.6%. ^1H NMR (400 MHz, Chloroform-*d*) δ 7.68 (d, J = 8.8 Hz, 1H), 7.03 (dd, J = 8.8, 2.6 Hz, 1H), 7.00 (d, J = 2.5 Hz, 1H), 6.76 (s, 1H), 6.29 (s, 1H), 5.72 (s, 2H), 3.67 (s, 2H), 3.65 – 3.62 (m, 2H), 3.62 – 3.52 (m, 8H), 3.48 – 3.42 (m, 2H), 3.36 (s, 3H), 1.61 (s, 9H). ^{13}C NMR (101 MHz, Chloroform-*d*) δ 177.18, 167.61, 164.47, 160.98, 160.67, 155.39, 149.58, 126.52, 114.11, 113.72, 112.80, 102.36, 71.88, 70.47, 70.33, 70.16, 69.54, 67.98, 58.90, 40.24, 39.70, 38.27, 29.15. HRMS $[\text{M}+\text{Na}]^+$ m/z calcd. for $[\text{C}_{25}\text{H}_{33}\text{N}_5\text{NaO}_7]^+$ 538.2272, found 538.2271.

3-(bromomethyl)-6-isopropyl-1,2,4,5-tetrazine (**iPrTz-Br**)

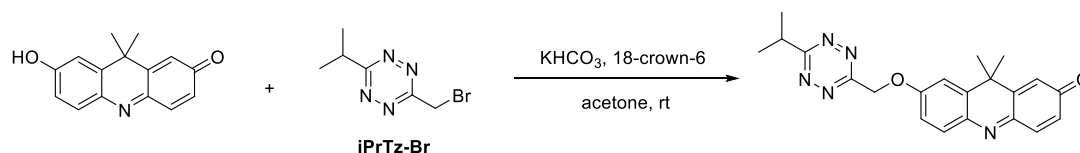


A mixture of isobutyrimidamide hydrochloride (613.0 mg, 5 mmol), 2-methoxyacetonitrile (1.5 mL, 20 mmol) and 3-mercaptopropionic acid (435 μL , 5 mmol) in ethanol (1.5 mL) was cooled to 0 $^\circ\text{C}$ under argon atmosphere. To this mixture was added dropwise hydrazine hydrate (3 mL, 60 mmol), then stirred at room temperature overnight. Upon completion, the reaction solution was cooled in ice water. An ice water solution of sodium nitrite (5.2 g, 75 mmol) was added, followed by slow addition of 1 M HCl during which the solution was stirred intensely and turned bright red, with gas evolved. Addition of 1M HCl continued until gas evolution ceased and the pH value turned 3–4. Then the mixture was extracted with DCM (70 mL \times 5), the combined organic phase was washed with brine, dried over sodium sulfate and concentrated in vacuo. The residue was purified on silica column chromatography to afford a liquid (452.9 mg, 54% yield). To a solution of the obtained compound (270.0 mg, 1.6 mmol) in DCM at -20 $^\circ\text{C}$ under argon atmosphere was added BBr_3 solution (1 M, 3.2 mL, 3.2

mmol) dropwise. The mixture was stirred at -20 °C for 3 h, then quenched with water and extracted with DCM. The combined organic phase was washed with brine, dried over Na₂SO₄ and evaporated under reduced pressure. The residue was purified on silica column chromatography to afford the desired product as a liquid (41 mg, 12% yield).

¹H NMR (400 MHz, Chloroform-*d*) δ 4.94 (s, 2H), 3.76 – 3.61 (m, 1H), 1.55 (s, 3H), 1.54 (s, 3H). ¹³C NMR (101 MHz, Chloroform-*d*) δ 174.34, 167.58, 34.57, 27.72, 21.36.

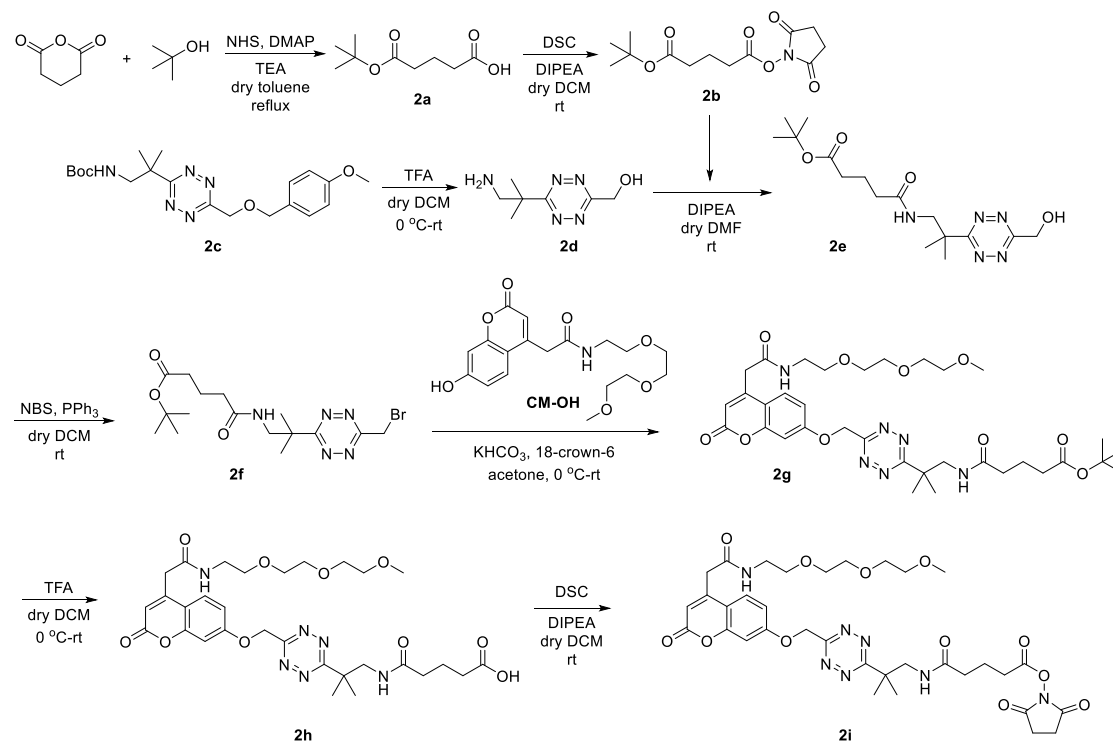
7-((6-isopropyl-1,2,4,5-tetrazin-3-yl)methoxy)-9,9-dimethylacridin-2(9H)-one (iPrTz-DAO)



DAO-OH (23.9 mg, 0.10 mmol), K₂CO₃ (30.0 mg, 0.30 mmol), 18-crown-6 (6.6 mg, 0.025 mmol), and acetone (1.0 mL) were added into a round bottom flask (5 mL) equipped with a magnetic stir bar. Cooled and stirred in an ice bath, the mixture was added dropwise with *iPrTz-Br* (26.1 mg, 0.12 mmol, dissolved in 0.2 mL acetone). The reaction mixture was brought to room temperature and stirred overnight. Purification by TLC plate afforded the product with the yield of 25.1%.

¹H NMR (400 MHz, Chloroform-*d*) δ 7.67 (d, *J* = 8.7 Hz, 1H), 7.40 (d, *J* = 9.7 Hz, 1H), 7.22 (d, *J* = 2.8 Hz, 1H), 7.08 (dd, *J* = 8.7, 2.7 Hz, 1H), 6.67 (d, *J* = 2.1 Hz, 1H), 6.64 (dd, *J* = 9.7, 2.1 Hz, 1H), 5.74 (s, 2H), 1.56 (d, *J* = 6.9 Hz, 6H), 1.53 (s, 6H). ¹³C NMR (101 MHz, CDCl₃) δ 187.15, 175.29, 165.35, 159.96, 151.14, 147.40, 141.69, 139.74, 137.49, 133.79, 131.37, 127.58, 113.48, 113.13, 68.00, 37.40, 34.51, 32.40, 21.25. HRMS [M+H]⁺ *m/z* calcd. for [C₂₁H₂₂N₅O₂]⁺ 376.1768, found 376.1765.

A novel bifunctional *t*BuTz linker chemistry was developed for conjugating the fluorophore to the oligonucleotide as well as quenching the fluorescence



Scheme S1. Development of a novel bifunctional *t*BuTz linker chemistry for conjugating the quenched fluorophore (CM) to the oligonucleotide.

5-(*tert*-butoxy)-5-oxopentanoic acid (**2a**)

Glutaric anhydride (1.0 g, 8.76 mmol) was added to toluene (5.0 mL) in a round bottom flask (50 mL) equipped with a magnetic stir bar. Then *N*-hydroxysuccinimide (300.4 mg, 2.61 mmol), 4-dimethylaminopyridine (DMAP, 107.5 mg, 0.88 mmol), *tert*-butanol (2.43 mL, 26.2 mmol), and triethylamine (360 μ L, 2.58 mmol) were added under stirring. The mixture was heated to reflux and stirred overnight. After cooling to room temperature, the mixture was diluted with ethylacetate (30 mL), washed by aqueous NaHSO₄ (5%, 30 mL \times 3) and brine (30 mL). The organic layer was dried over Na₂SO₄ and concentrated via rotary evaporation. Purification by silica gel chromatography (PE/EA = 3/1) afforded the product as a colorless oil (527.6 mg, 32.0%).

¹H NMR (400 MHz, Chloroform-*d*) δ 2.42 (t, *J* = 7.4 Hz, 2H), 2.31 (t, *J* = 7.3 Hz, 2H),

1.92 (p, $J = 7.2$ Hz, 2H), 1.45 (s, 9H).

tert-butyl (2,5-dioxopyrrolidin-1-yl) glutarate (2b)

2a (527.6 mg, 2.80 mmol) and *N,N*-disuccinimidyl carbonate (DSC, 1075.9 mg, 4.20 mmol) were added into a round bottom flask (25 mL) equipped with a magnetic stir bar, dissolved by dichloromethane (DCM, 10 mL). *N,N*-diisopropylethylamine (DIPEA, 928 μ L, 5.60 mmol) was then added while stirring. After overnight reaction at room temperature, the mixture was concentrated via rotary evaporation. Purification by silica gel chromatography (PE/EA = 3/1) afforded the product as a colorless oil (451.7 mg, 56.6%), which turned to waxy solid in the refrigerator.

^1H NMR (400 MHz, Chloroform-*d*) δ 2.84 (s, 4H), 2.69 (t, $J = 7.4$ Hz, 2H), 2.37 (t, $J = 7.3$ Hz, 2H), 2.08 – 1.96 (m, 2H), 1.45 (s, 9H).

tert-butyl 5-((2-(6-(hydroxymethyl)-1,2,4,5-tetrazin-3-yl)-2-methylpropyl)amino)-5-oxopentanoate (2e)

2c (112.9 mg, 0.28 mmol) was dissolved in anhydrous DCM (1.6 mL), cooled in ice bath. Trifluoroacetic acid (TFA, 400 μ L) was added dropwise under stirring. The mixture was brought to room temperature and stirred for 1 h. After concentrated by rotary evaporation and dried *in vacuo*, the residue was dissolved by anhydrous *N,N*-dimethylformamide (DMF, 1.0 mL). DIPEA (93 μ L, 0.56 mmol) and **2b** (95.8 mg, 0.34 mmol) was added successively under stirring. After overnight reaction at room temperature, the mixture was diluted with ethylacetate (15 mL), then washed by brine (15 mL \times 3). The organic layer was dried over Na_2SO_4 and concentrated via rotary evaporation. Purification by silica gel chromatography (PE/EA = 1/1) afforded the product as a pink oil (40.0 mg, 40.4%).

^1H NMR (400 MHz, Chloroform-*d*) δ 6.21 (s, 1H), 5.29 (s, 2H), 3.71 (d, $J = 6.6$ Hz, 2H), 3.49 (s, 1H), 2.21 (t, $J = 7.2$ Hz, 2H), 2.14 (t, $J = 7.4$ Hz, 2H), 1.86 – 1.77 (m, 2H), 1.61 (s, 6H), 1.42 (s, 9H).

tert-butyl 5-((2-(6-(bromomethyl)-1,2,4,5-tetrazin-3-yl)-2-methylpropyl)amino)-5-

oxopentanoate (2f)

A round bottom flask (10 mL) equipped with a magnetic stir bar was charged with **2e** (32.7 mg, 0.09 mmol), *N*-bromosuccinimide (24.7 mg, 0.14 mmol) and triphenylphosphine (18.3 mg, 0.07 mmol). Under the protection of Ar, anhydrous DCM (1.0 mL) was added. The mixture was stirred at room temperature for 3 h, then purified by TLC plate, affording the product as a pink oil (22.7 mg, 58.7%).

¹H NMR (400 MHz, Chloroform-*d*) δ 6.21 (s, 1H), 4.96 (s, 2H), 3.74 (d, *J* = 6.6 Hz, 2H), 2.22 (t, *J* = 7.2 Hz, 2H), 2.16 (t, *J* = 7.4 Hz, 2H), 1.90 – 1.78 (m, 2H), 1.60 (s, 6H), 1.42 (s, 9H).

tert-butyl 5-((2-methyl-2-(6-(((2-oxo-4-(12-oxo-2,5,8-trioxa-11-azatridecan-13-yl)-2H-chromen-7-yl)oxy)methyl)-1,2,4,5-tetrazin-3-yl)propyl)amino)-5-oxopentanoate (2g)

CM-OH (13.0 mg, 35.6 μmol), KHCO₃ (10.7 mg, 106.8 μmol), 18-crown-6 (2.4 mg, 8.9 μmol), and acetone (1.0 mL) were added into a round bottom flask (5 mL) equipped with a magnetic stir bar. Cooled and stirred in an ice bath, the mixture was added dropwise with **2f** (9.9 mg, 23.7 μmol, dissolved in 0.2 mL acetone). The reaction mixture was brought to room temperature and stirred overnight. Purification by TLC plate afforded **2g** as a red solid (8.3 mg, 50.0%).

¹H NMR (400 MHz, Chloroform-*d*) δ 7.69 (d, *J* = 8.8 Hz, 1H), 7.04 (dd, *J* = 8.8, 2.5 Hz, 1H), 7.01 (d, *J* = 2.6 Hz, 1H), 6.30 (s, 1H), 5.74 (s, 2H), 3.70 – 3.51 (m, 14H), 3.46 (t, *J* = 5.1 Hz, 2H), 3.37 (s, 3H), 2.22 (t, *J* = 7.1 Hz, 2H), 2.16 (t, *J* = 7.4 Hz, 2H), 1.83 (t, *J* = 7.3 Hz, 2H), 1.61 (s, 6H), 1.42 (s, 9H).

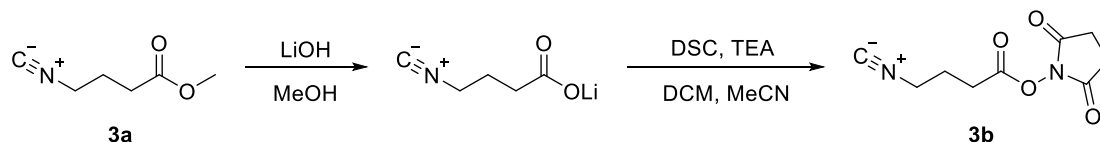
2,5-dioxopyrrolidin-1-yl 5-((2-methyl-2-(6-(((2-oxo-4-(12-oxo-2,5,8-trioxa-11-azatridecan-13-yl)-2H-chromen-7-yl)oxy)methyl)-1,2,4,5-tetrazin-3-yl)propyl)amino)-5-oxopentanoate (2i)

2g (8.3 mg, 11.8 μmol) was dissolved in anhydrous DCM (400 μL), cooled in ice bath. TFA (100 μL) was added dropwise under stirring. The mixture was brought to room temperature and stirred for 3 h. After concentrated by rotary evaporation and dried *in*

vacuo, the residue was dissolved in anhydrous DCM (500 μ L). The solution was added with DIPEA (9.8 μ L, 59.0 μ mol), stirred for 5 min at room temperature, then added slowly with DSC (6.0 mg, 23.6 μ mol). After stirring under room temperature for 3 h, purification by TLC plate afforded **2i** as a red solid (3.2 mg, 36.6%).

^1H NMR (400 MHz, Chloroform-*d*) δ 7.69 (d, J = 8.8 Hz, 1H), 7.07 – 6.98 (m, 2H), 6.77 (s, 1H), 6.46 (t, J = 5.9 Hz, 1H), 6.30 (s, 1H), 5.73 (s, 2H), 3.75 (d, J = 6.5 Hz, 2H), 3.69 – 3.53 (m, 12H), 3.49 – 3.41 (m, 2H), 3.37 (s, 3H), 2.84 (s, 4H), 2.59 (t, J = 6.7 Hz, 2H), 2.28 – 2.18 (m, 2H), 2.07 – 1.97 (m, 2H), 1.61 (s, 6H). HRMS $[\text{M}+\text{Na}]^+$ m/z calcd. for $[\text{C}_{34}\text{H}_{43}\text{N}_7\text{NaO}_{12}]^+$ 764.2862, found 764.2867.

2,5-dioxopyrrolidin-1-yl 4-isocyanobutanoate (**3b**)



3a (127.1 mg, 1.0 mmol) was dissolved in MeOH (3 mL), then added with LiOH·H₂O (63.2 mg, 1.5 mmol), and stirred at room temperature for 2 h. After removing the solvent by rotary evaporation, the residue was dissolved by DCM (2 mL) and MeCN (2 mL), then added with DSC (512.3 mg, 2.0 mmol) and TEA (280 μ L, 2.0 mmol). The mixture was stirred at room temperature for 2 h, then concentrated via rotary evaporation. Purification by silica gel chromatography afforded the product as a white solid (126.6 mg, 60.3%).

^1H NMR (400 MHz, CDCl₃) δ 3.57 (t, J = 6.4 Hz, 2H), 2.94 – 2.78 (m, 6H), 2.14 (d, J = 6.6 Hz, 2H). ^{13}C NMR (101 MHz, CDCl₃) δ 169.01, 167.55, 157.94, 157.88, 157.83, 40.51, 40.44, 40.38, 27.82, 25.70, 24.42.

3. Absorption and fluorescence emission spectra of *t*BuTz-caged probes before and after cleavage reaction

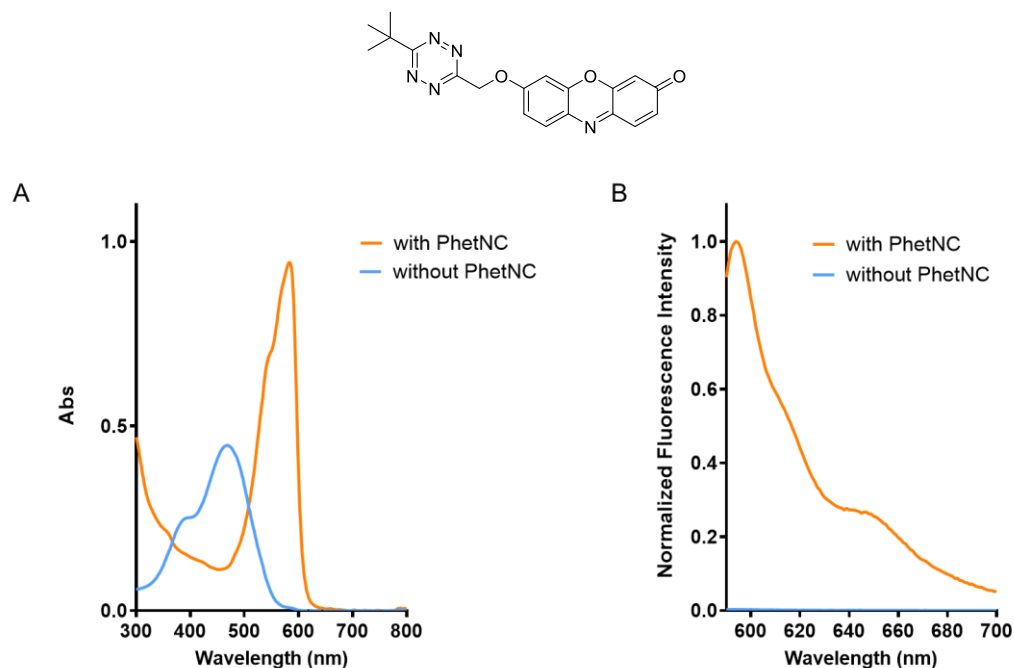


Figure S1. (A) UV-Vis absorption spectra of probe **1a** (10 μ M, 50% DMSO in PBS pH 7.4) before (blue) and after (red) cleavage reaction with **PhetNC**. (B) Normalized fluorescence emission spectra of probe **1a** (2 μ M, 50% DMSO in PBS pH 7.4) before (blue) and after (red) cleavage reaction with **PhetNC**, with the excitation wavelength of 584 nm. The solution of intact probe **1a** was obtained from direct dilution of the stock solution (1 mM in DMSO) to the indicated concentration. The solution after cleavage was obtained from the completed reaction between probe **1a** (100 μ M) and **PhetNC** (1 mM) in 50% DMSO/PBS pH 7.4 as monitored by LC-MS, which was diluted to the indicated concentration.

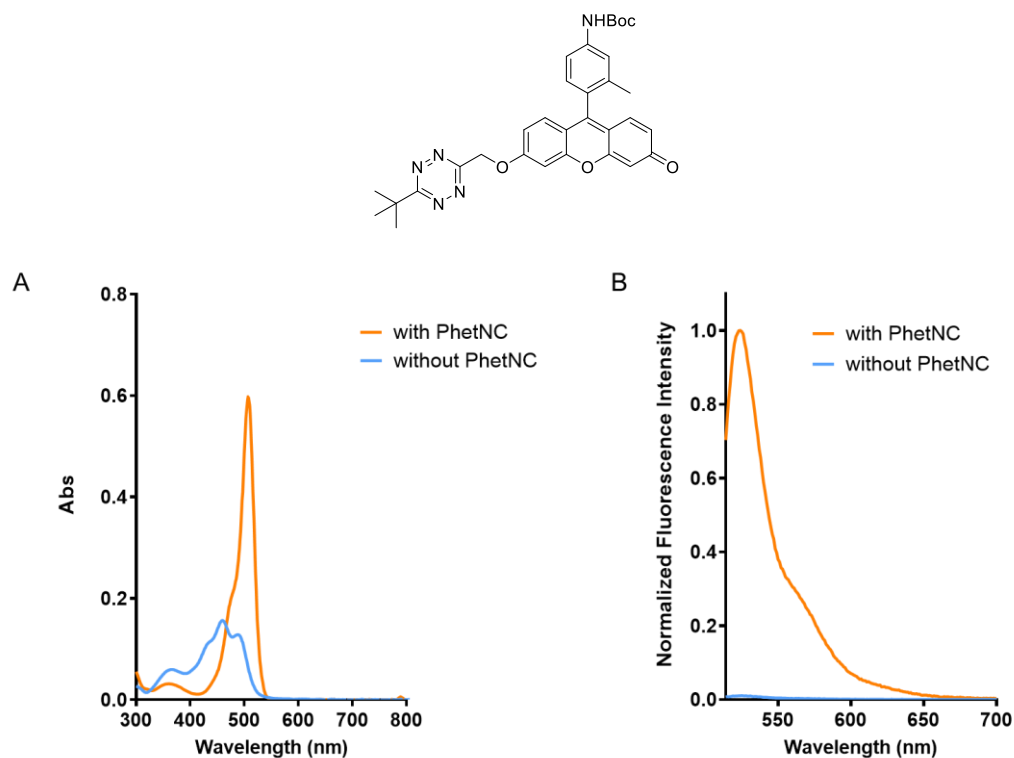


Figure S2. (A) UV-Vis absorption spectra of probe **1b** (10 μ M, 50% DMSO in PBS pH 7.4) before (blue) and after (red) cleavage reaction with **PhetNC**. (B) Normalized fluorescence emission spectra of probe **1b** (2 μ M, 50% DMSO in PBS pH 7.4) before (blue) and after (red) cleavage reaction with **PhetNC**, with the excitation wavelength of 508 nm. The solution of intact probe **1b** was obtained from direct dilution of the stock solution (1 mM in DMSO) to the indicated concentration. The solution after cleavage was obtained from the completed reaction between probe **1b** (100 μ M) and **PhetNC** (1 mM) in 50% DMSO/PBS pH 7.4 as monitored by LC-MS, which was diluted to the indicated concentration.

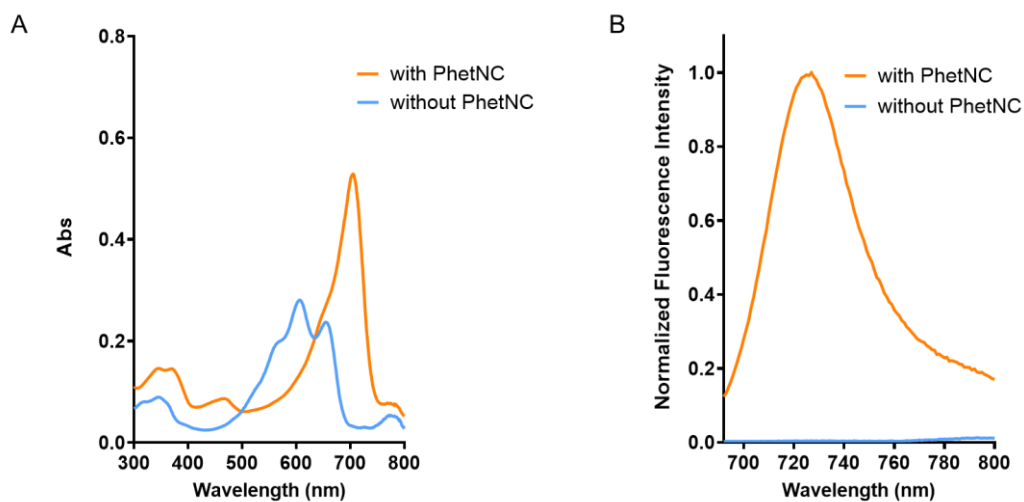
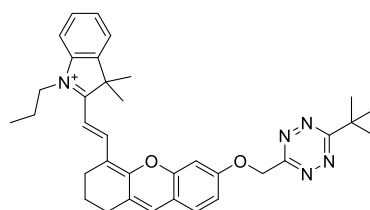


Figure S3. (A) UV-Vis absorption spectra of probe **1c** (10 μM , 50% DMSO in PBS pH 7.4) before (blue) and after (red) cleavage reaction with **PhetNC**. (B) Normalized fluorescence emission spectra of probe **1c** (2 μM , 50% DMSO in PBS pH 7.4) before (blue) and after (red) cleavage reaction with **PhetNC**, with the excitation wavelength of 680 nm. The solution of intact probe **1c** was obtained from direct dilution of the stock solution (1 mM in DMSO) to the indicated concentration. The solution after cleavage was obtained from the completed reaction between probe **1c** (100 μM) and **PhetNC** (1 mM) in 50% DMSO/PBS pH 7.4 as monitored by LC-MS, which was diluted to the indicated concentration.

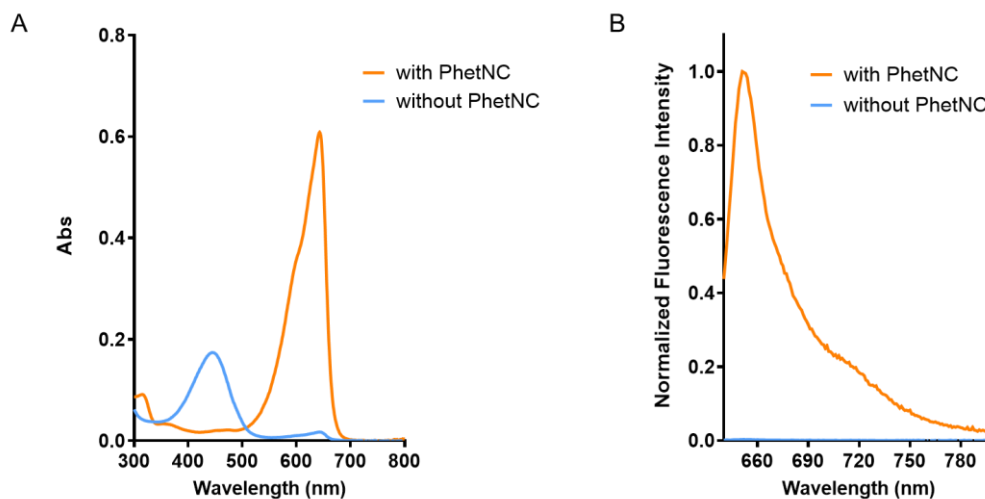
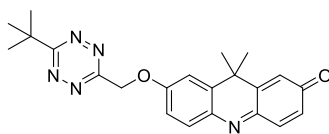
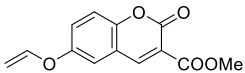
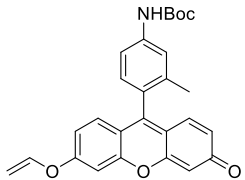
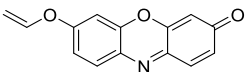
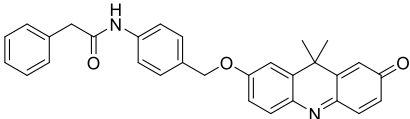
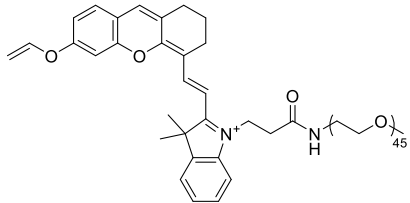


Figure S4. (A) UV-Vis absorption spectra of probe **1d** (10 μ M, 50% DMSO in PBS pH 7.4) before (blue) and after (red) cleavage reaction with **PhetNC**. (B) Normalized fluorescence emission spectra of probe **1d** (2 μ M, 50% DMSO in PBS pH 7.4) before (blue) and after (red) cleavage reaction with **PhetNC**, with the excitation wavelength of 630 nm. The solution of intact probe **1d** was obtained from direct dilution of the stock solution (1 mM in DMSO) to the indicated concentration. The solution after cleavage was obtained from the completed reaction between probe **1d** (100 μ M) and **PhetNC** (1 mM) in 50% DMSO/PBS pH 7.4 as monitored by LC-MS, which was diluted to the indicated concentration.

4. Fluorescence quenching efficiency of vinyl ether in the literature

Table S1. Structure and fluorescence turn-on fold of previously reported vinyl ether quenched probes containing the same fluorophores employed in this work.

Quenched probe*	Fluorescence turn-on fold	Reference
	162	<i>J. Am. Chem. Soc.</i> , 2016, 138 , 11429-11432.
	11	<i>J. Am. Chem. Soc.</i> , 2016, 138 , 11429-11432.
	32.6	PCT Int. Appl. (2017), WO 2017046602 A1 20170323.
	8.5	<i>Bioconjug. Chem.</i> , 2008, 19 , 1707-1718.
	47	<i>Angew. Chem. Int. Ed.</i> , 2020, 59 , 7168-7172.

*Vinyl ether quenched DAO has not been reported in the literature.

5. The stability and activation of quenched probes in buffer and cell culture medium

Fluorescence increased significantly upon the addition of excess **PhetNC**, no matter before or after 2h incubation of the quenched probes.

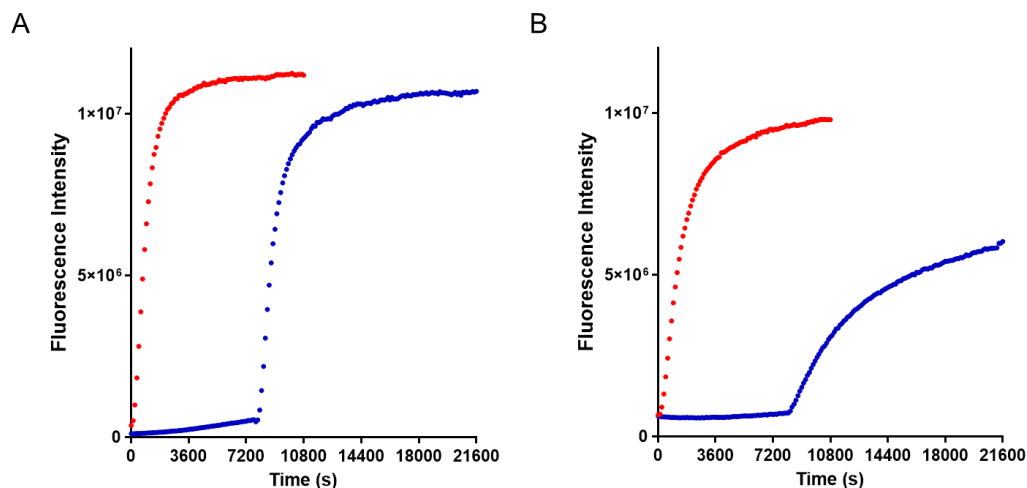


Figure S5. The fluorescence signal of probe **1c** ($2 \mu\text{M}$) activated by the addition of **PhetNC** (1 mM) with (blue dots) or without (red dots) pre-incubation in (A) PBS buffer (10% DMSO) or (B) cell culture medium DMEM (10% FBS, 10% DMSO). The fluorescence signal was collected at $37 \text{ }^\circ\text{C}$ by kinetics program with time increment of 150 s ($\lambda_{\text{ex}} = 680 \text{ nm}$, $\lambda_{\text{em}} = 717 \text{ nm}$).

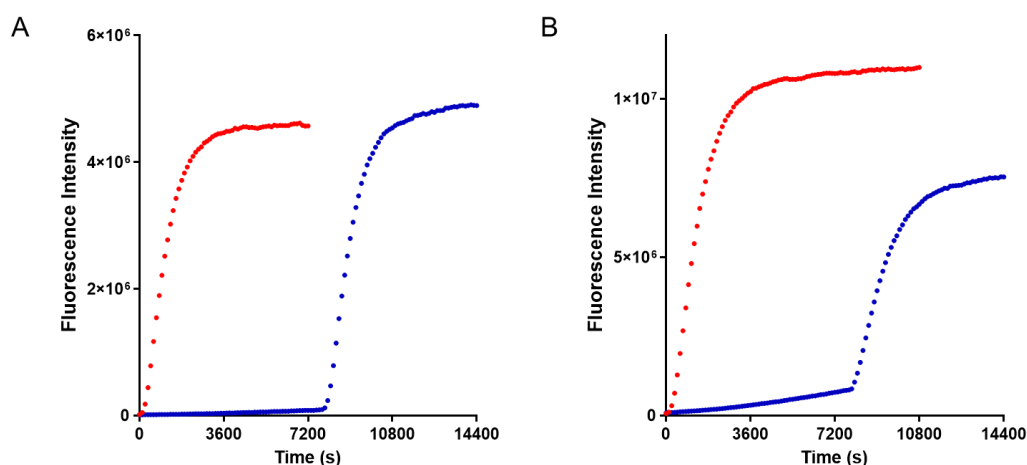


Figure S6. The fluorescence signal of probe **1d** ($2 \mu\text{M}$) activated by the addition of **PhetNC** (1 mM) with (blue dots) or without (red dots) pre-incubation in (A) PBS buffer (10% DMSO) or (B) cell culture medium DMEM (10% FBS, 10% DMSO). The fluorescence signal was collected at $37 \text{ }^\circ\text{C}$ by kinetics program with time increment of 150 s ($\lambda_{\text{ex}} = 630 \text{ nm}$, $\lambda_{\text{em}} = 646 \text{ nm}$).

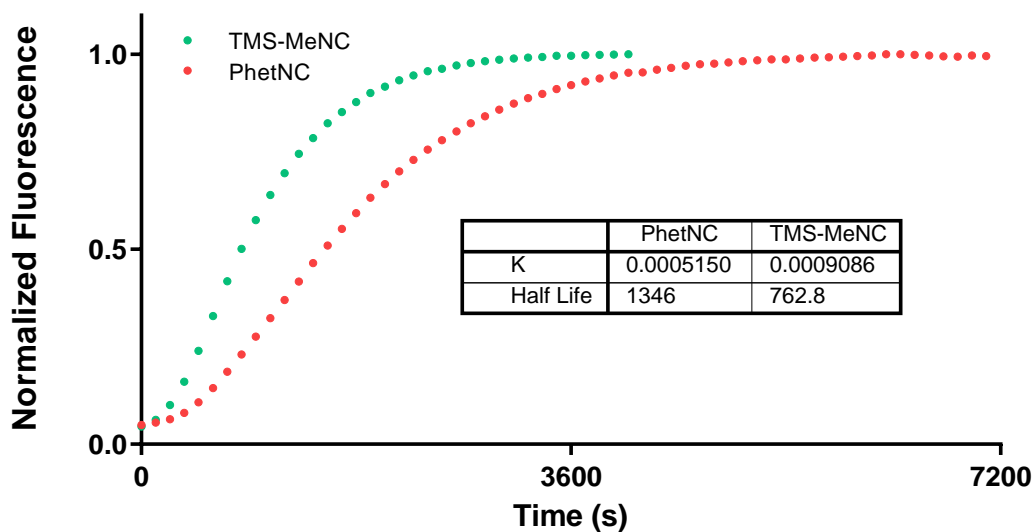


Figure S7. *tBuTz-FL* (2 μM) was activated by **TMS-MeNC** (1 mM) or **PhetNC** (1 mM) under the same conditions (in 10% DMSO-PBS, 37 $^{\circ}\text{C}$). The k value for **TMS-MeNC** was about 1.8-fold higher than the k value for **PhetNC**.

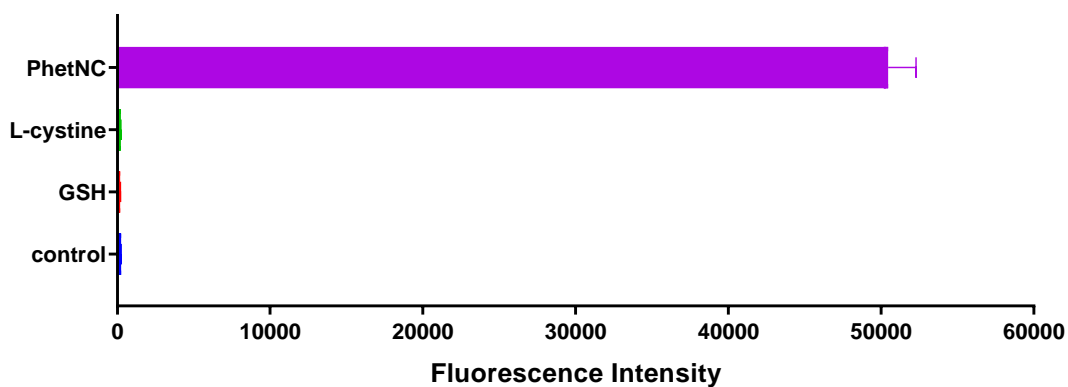


Figure S8. The response of *tBuTz-FL* (2 μM) towards **PhetNC**, GSH, and L-cystine (all 1 mM) under the same incubation conditions (in 10% DMSO-PBS, 37 $^{\circ}\text{C}$ for 3 h). Significantly enhanced fluorescence intensity was only induced by **PhetNC**, while only background level fluorescence was observed for GSH and L-cystine, confirming the specificity of *tBuTz-FL* towards **PhetNC**.

6. Fluorophore release monitored by LC-MS

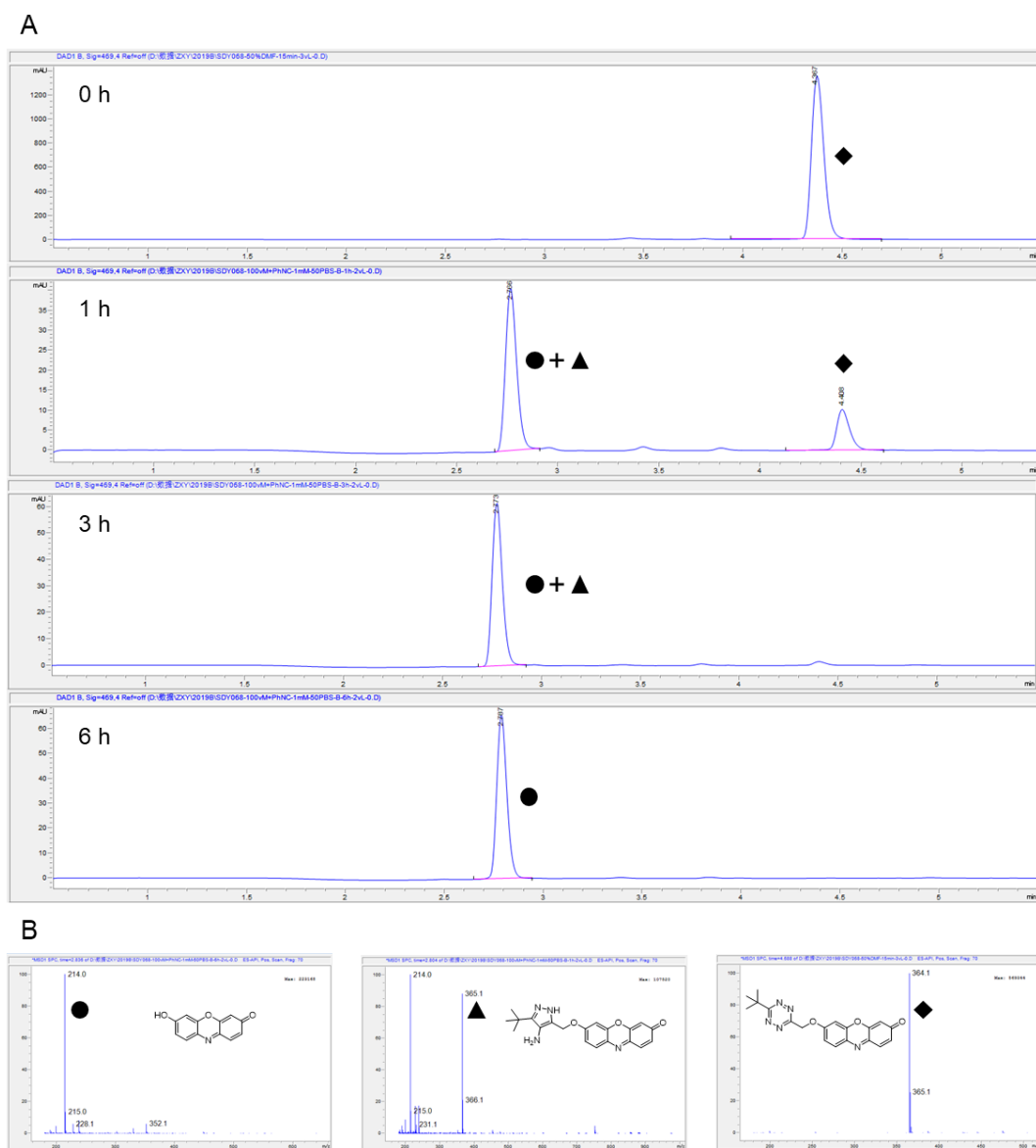


Figure S9. (A) LC profile of reaction progress between *t*BuTz-RSF (100 μ M) and PhetNC (1 mM) in 50% DMSO/PBS at 37 $^{\circ}$ C; (B) MS of the product RSF-OH (●), the intermediate (▲), and the intact probe *t*BuTz-RSF (♦).

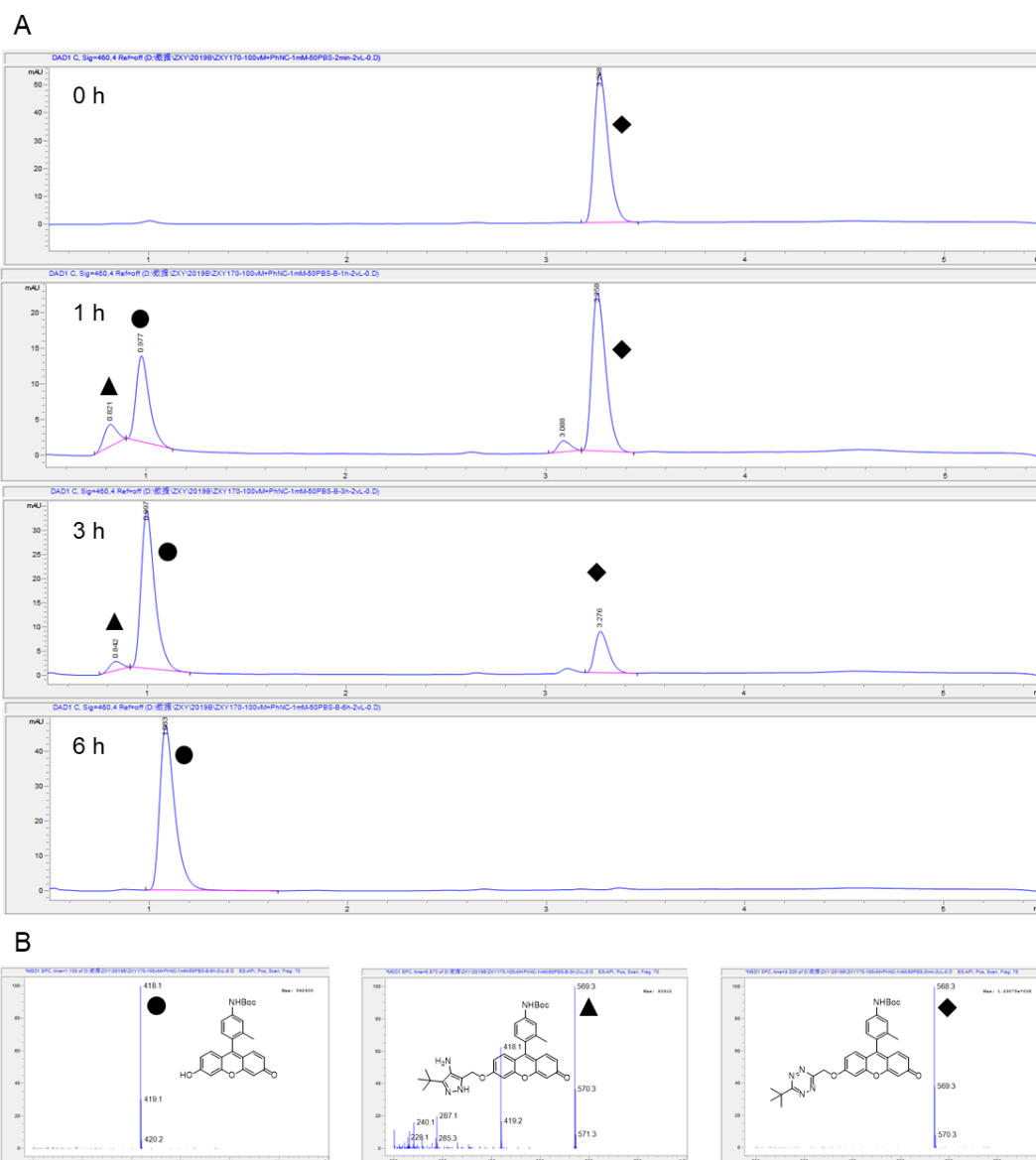


Figure S10. (A) LC profile of reaction progress between *t*BuTz-FL (100 μ M) and PhetNC (1 mM) in 50% DMSO/PBS at 37 $^{\circ}$ C; (B) MS of the product FL-OH (●), the intermediate (▲), and the intact probe *t*BuTz-FL (♦).

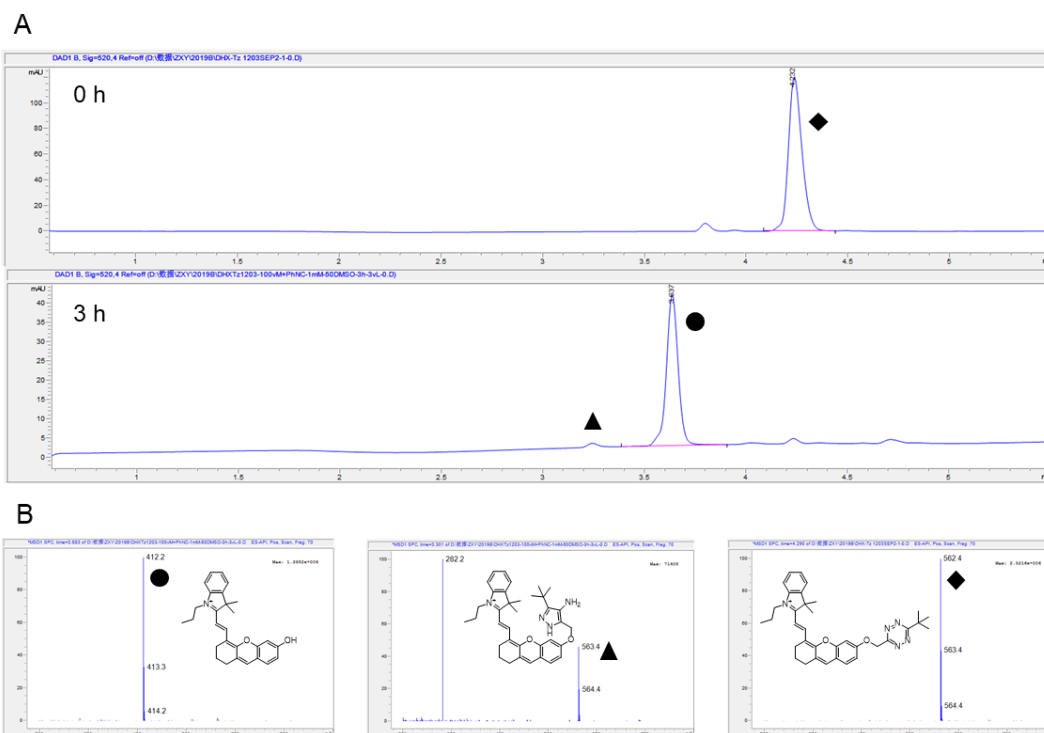


Figure S11. (A) LC profile of reaction progress between *t*BuTz-DHX (100 μ M) and PhetNC (1 mM) in 50% DMSO/PBS at 37 $^{\circ}$ C; (B) MS of the product DHX-OH (●), the intermediate (▲), and the intact probe *t*BuTz-DHX (◆).

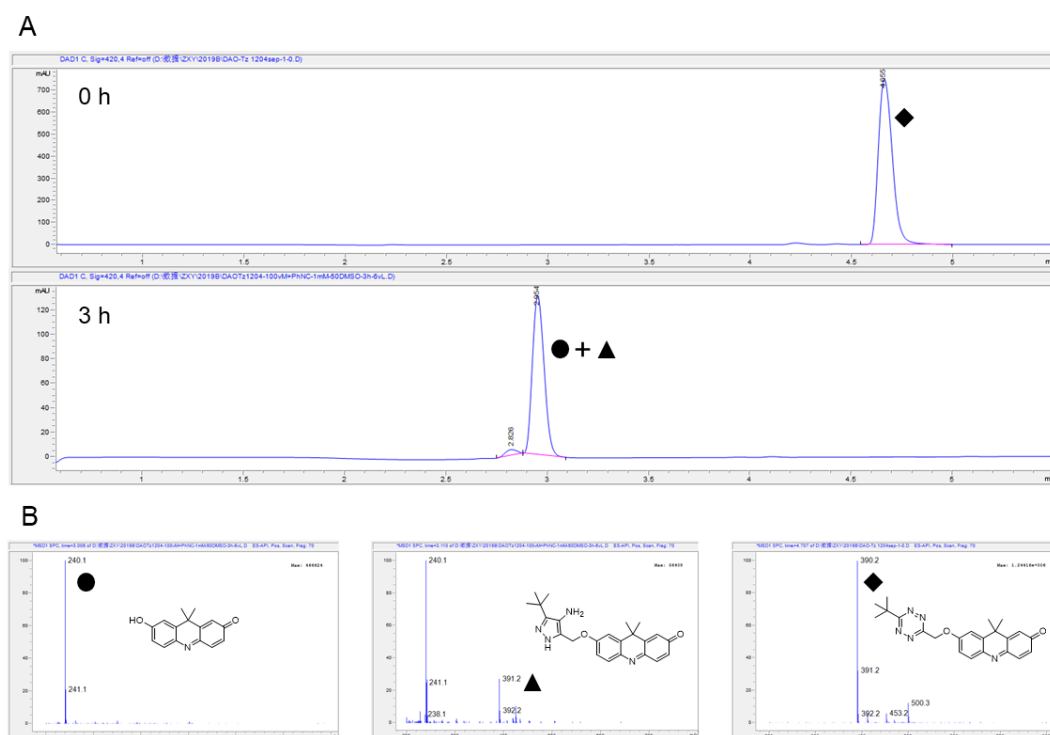
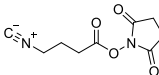
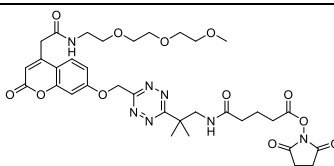
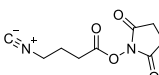
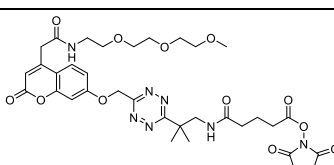


Figure S12. (A) LC profile of reaction progress between *t*BuTz-DAO (100 μ M) and PhetNC (1 mM) in 50% DMSO/PBS at 37 $^{\circ}$ C; (B) MS of the product DAO-OH (●), the intermediate (▲), and the intact probe *t*BuTz-DAO (◆).

7. Preparation and characterization of oligonucleotide probes

A set of oligoDNA sequences were designed, including the template sequence **1C**, the probe sequences **1A** and **1B** bearing terminal amino group for further modification. Probe **1A-NC** and **1B-CM** were synthesized straightforward via NHS chemistry, carefully purified through HPLC, and identified by LC-MS. Both the NHS esters formed flexible linkage structure between the reaction partner and the nucleic acid sequence, providing the necessary conformational flexibility for the molecular interaction.

Table S2. Probe sequences and modification structures

Name	Type	Sequence (5'- 3')	Modification
1A-NC	DNA	ACT CTT CCC CAC /3AmMC6/	
1B-CM		/5AmMC6/ CCT ACA GCG C	
r1A-NC	Phosphorothioated 2'-O-methyl RNA	/5AmMC6/ mUmC*mU mA*mCmA* mGmG*mG mU*mA	
r1B-CM		mCmA*mC mA*mAmA* mUmU*mC mG*mG /3AmMC6/	

/3AmMC6 /: 3' amino modifier C6; /5AmMC6 /: 5' amino modifier C6.

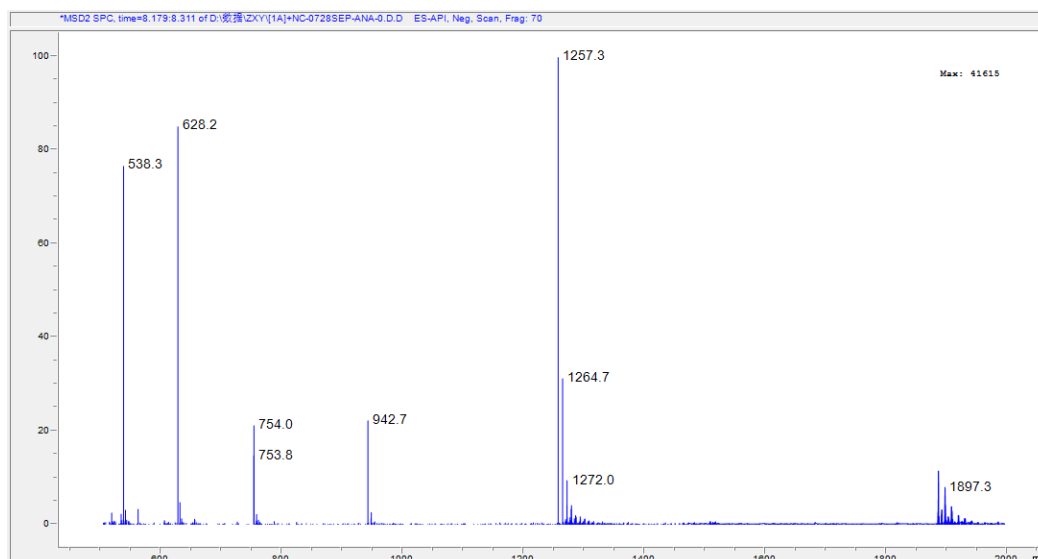
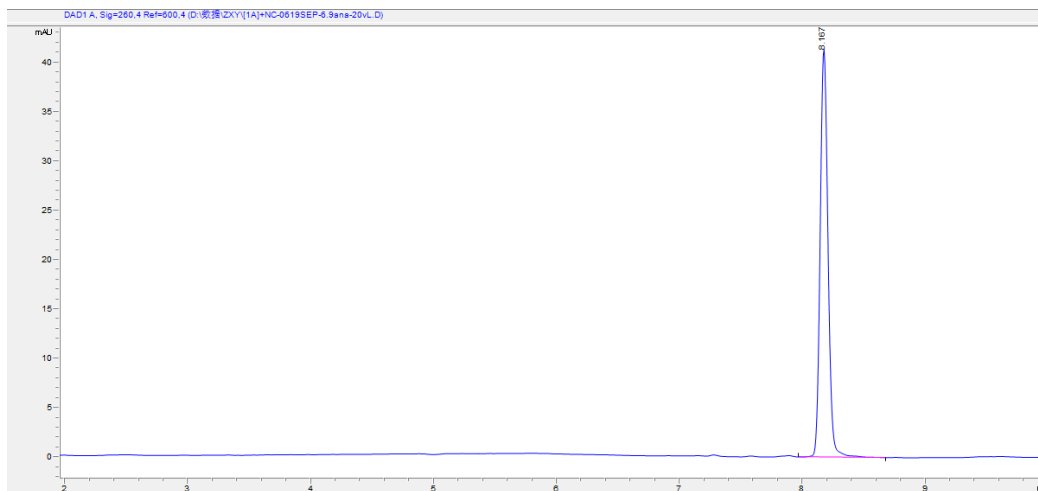
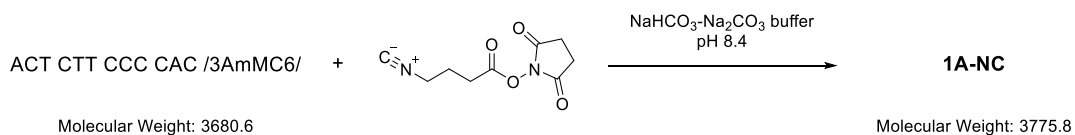
'm_': 2' O-methyl RNA bases; 'm_*': phosphorothioated 2'-O-methyl RNA bases.

Table S3. Template sequences

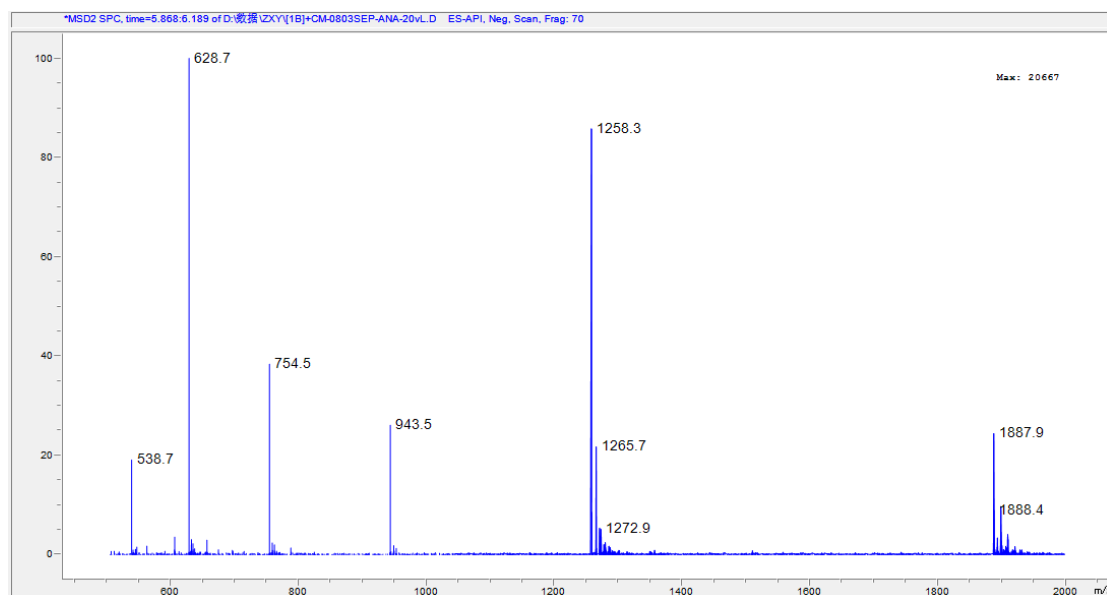
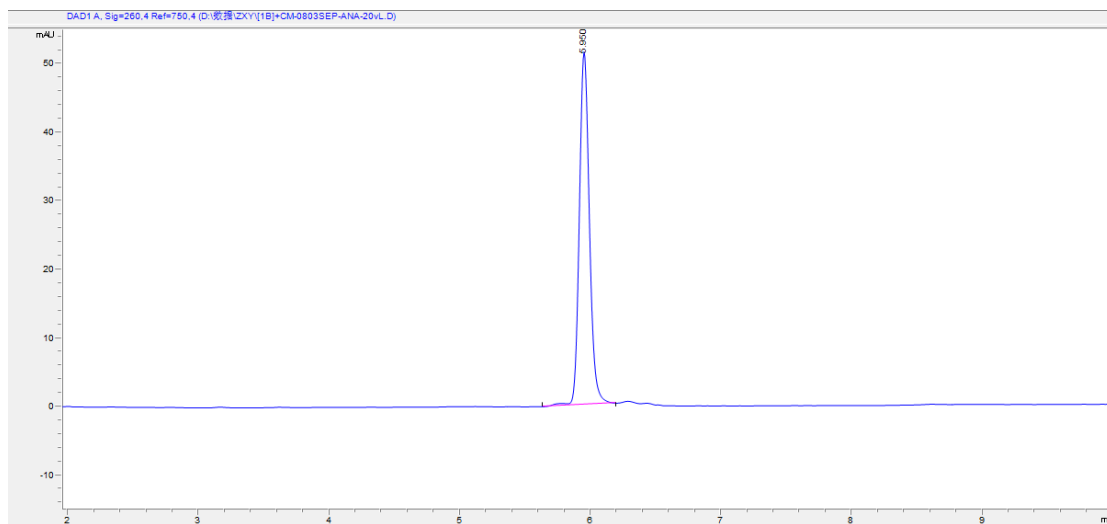
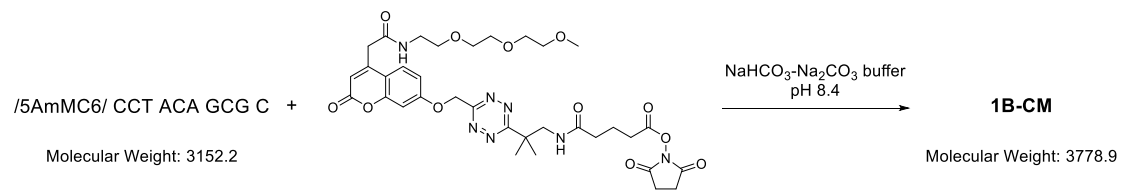
Name	Type	Sequence (5'- 3')
1C	DNA	GCG CTG TAG GGT GGG GAA GAG T
r1C (miR-10b)	RNA	UAC CCU GUA GAA CCG AAU UUG UG

Oligonucleotide sequence bearing terminal amino group was dissolved in NaHCO₃-Na₂CO₃ buffer (0.1 M, pH 8.4) to the final concentration of 0.1 mM. A specific NHS ester (10 mM stock solution in DMF) was then added to the final concentration of 3 mM. The reaction was mixed well, kept under room temperature for 3-6 h while monitored by LC-MS. A Phenomenex Clarity Oligo-RP column (100 × 2 mm, 3 μm) was used for LC-MS, utilizing TEA/HFIP/H₂O (0.4/30/1000, v/v/v) as mobile phase A and methanol as mobile phase B. The product was carefully purified via LC-MS, lyophilized, and stored at -80 °C in aliquots avoiding freeze-thaw cycle.

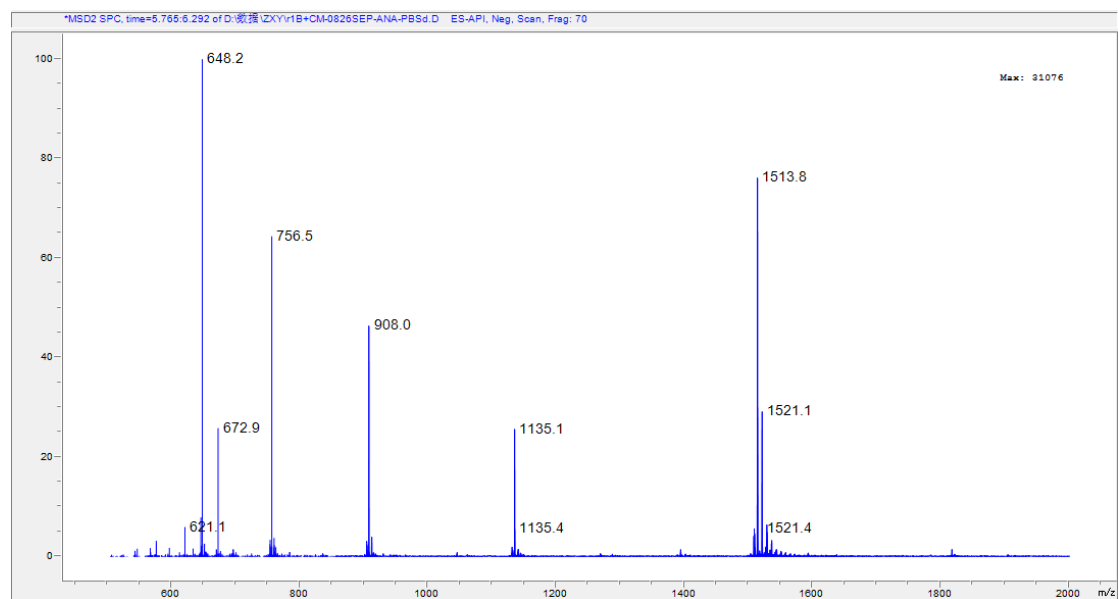
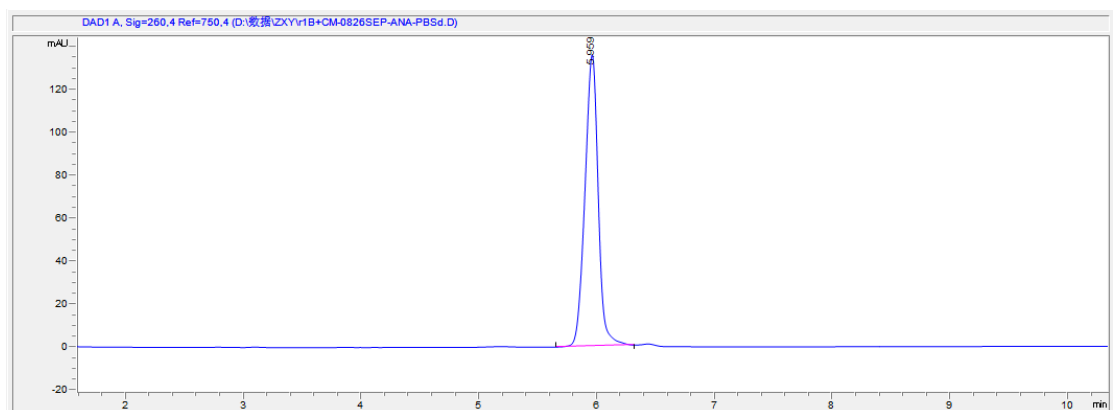
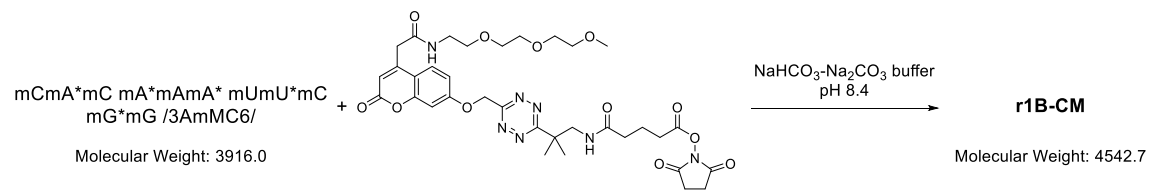
Characterization of 1A-NC



Characterization of 1B-CM



Characterization of r1B-CM



8. Fluorescence turn-on via DNA templated cleavage

A solution of **1A-NC** (100 nM) and **1B-CM** (100 nM) in 100 mM Tris-HCl buffer (pH 8.4) was added with DNA template sequence **1C** (final concentration at 100 nM), well mixed, and incubated at 37 °C. The fluorescence intensity was measured over time ($\lambda_{\text{ex}} = 373 \text{ nm}$, $\lambda_{\text{em}} = 464 \text{ nm}$) by a FluoroMax-4 fluorometer (Horiba Jobin Yvon), commenced immediately upon the addition of **1C**.

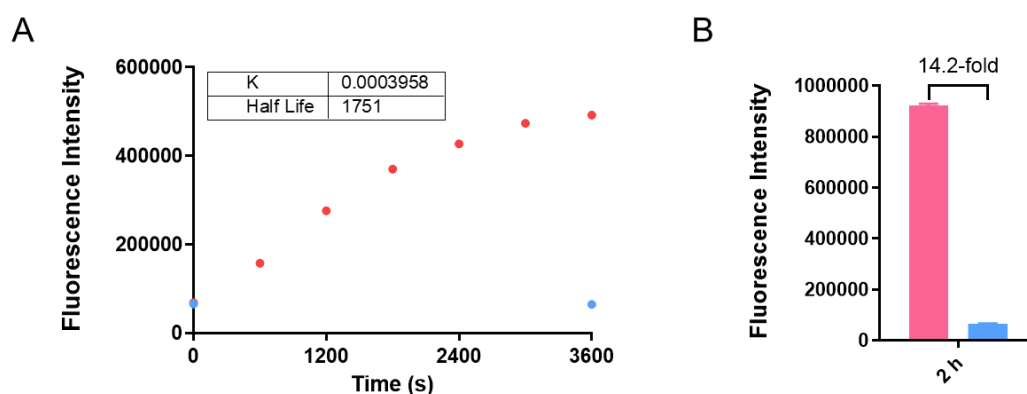


Figure S13. (A) The fluorescence increase of DNA templated cleavage over time (red dots), in contrast with the control group (in the absence of **1A-NC**, blue dots). (B) The fluorescence intensity at 2 h exhibited 14.2-fold turn-on (red bar), compared with the control group (in the absence of **1A-NC**, blue bar).

In Tris-HCl buffer (pH 8.4), a mixture of **1A-NC** and **1B-CM** produced rapid fluorescence enhancement at an equimolar concentration as low as 100 nM in the presence of **1C** (100 nM). No pronounced fluorescence was observed without **1A-NC**, indicating the specificity of the fluorogenic process.

9. Fluorescence turn-on via RNA templated cleavage

A solution of **r1A-NC** (100 nM) and **r1B-CM** (100 nM) in 100 mM Tris-HCl buffer (pH 8.4) was added with RNA template sequence **r1C** (final concentration at 100 nM), well mixed, and incubated at 37 °C. The fluorescence intensity was measured on a TECAN Spark multifunctional microplate reader by kinetics program with time increment of 15 min ($\lambda_{\text{ex}} = 373 \text{ nm}$, $\lambda_{\text{em}} = 464 \text{ nm}$, both with bandwidth of 20 nm), commenced immediately upon the addition of **r1C**. Control groups were conducted under the same conditions in the absence of **r1A-NC** and/or **r1C**.

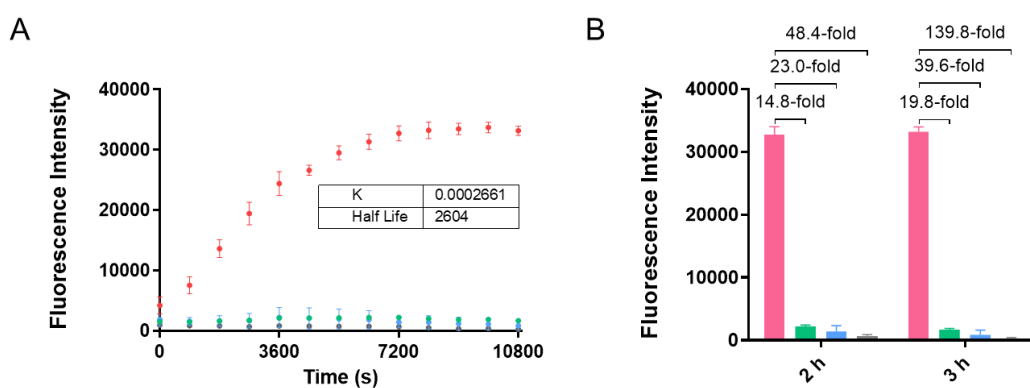


Figure S14. (A) The fluorescence increase of RNA templated cleavage over time (red dots), in contrast with the control groups (in the absence of **r1C**, green dots; in the absence of **r1A-NC**, blue dots; in the absence of **r1A-NC** and **r1C**, grey dots). (B) The fluorescence intensity at 2 h and 3 h for RNA templated cleavage (red bars), compared with the control groups (in the absence of **r1C**, green bars; in the absence of **r1A-NC**, blue bars; in the absence of **r1A-NC** and **r1C**, grey bars).

Note: for the top-reading mode of the plate reader, the measured fluorescence intensity is affected by not only the fluorophore concentration but also the sample volume. Once the sample volume changed, the distance between the sample and the detection optics also changed, thus affected the sensitivity of detection. In our assays, the sample volume decreased due to the unavoidable evaporation during incubation in the plate reader (37 °C for 3 h with no lid), then the distance between the sample and the detection optics increased, affecting the detection sensitivity (presumably decreased in our case).

10. The stability and activation of *i*PrTz-DAO

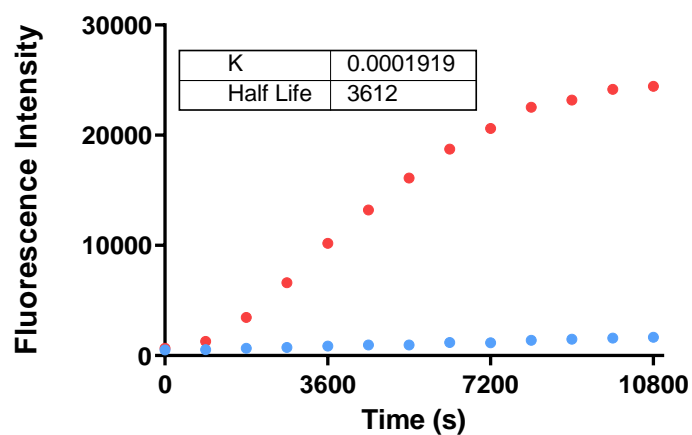


Figure S15. The fluorescence signal of *i*PrTz-DAO (0.5 μ M) over time (0-3 h) in the presence (red dots) or absence (blue dots) of TCO-OH (5.0 μ M) in 10% DMSO/PBS (pH 7.2) at 37 $^{\circ}$ C. The fluorescence signal was collected on a TECAN Spark multifunctional microplate reader by kinetics program with time increment of 15 min ($\lambda_{\text{ex}} = 620$ nm, $\lambda_{\text{em}} = 660$ nm, both with bandwidth of 20 nm).

11. Mutually orthogonal release of fluorophores involving DNA template

In 10% DMSO/PBS (pH 7.2), reagents involved in two mutually orthogonal cleavage reactions were added as indicated below designed for four groups. The mixture was vortexed and incubated at 37 °C. The fluorescence signal of CM ($\lambda_{\text{ex}} = 373 \text{ nm}$, $\lambda_{\text{em}} = 464 \text{ nm}$) and DAO ($\lambda_{\text{ex}} = 630 \text{ nm}$, $\lambda_{\text{em}} = 646 \text{ nm}$) was measured in a row at indicated time point by a FluoroMax-4 fluorometer (Horiba Jobin Yvon).

Reagent	Conc.	+NC +TCO	+NC -TCO	-NC +TCO	-NC -TCO
1C	100 nM	+	+	+	+
1B-CM	100 nM	+	+	+	+
<i>i</i>PrTz-DAO	0.5 μM	+	+	+	+
1A-NC	100 nM	+	+	-	-
TCO-OH	5.0 μM	+	-	+	-

Attendance reagent (+), or no reagent (-)

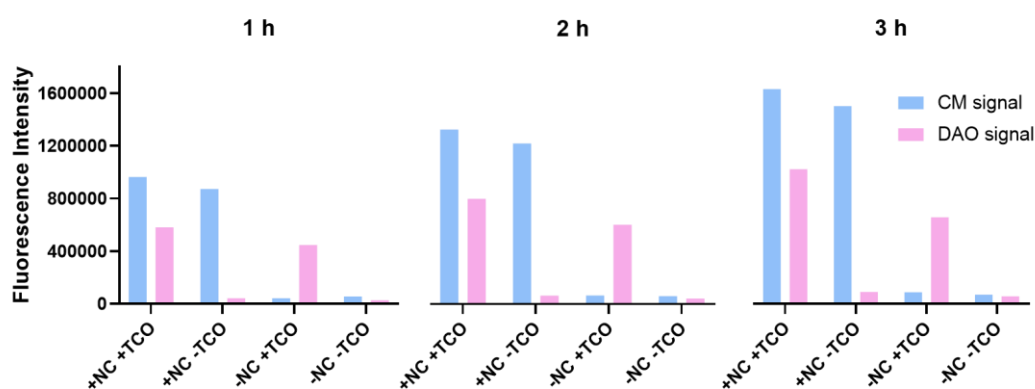


Figure S16. The fluorescence intensity of CM and DAO in each group at indicated time point.

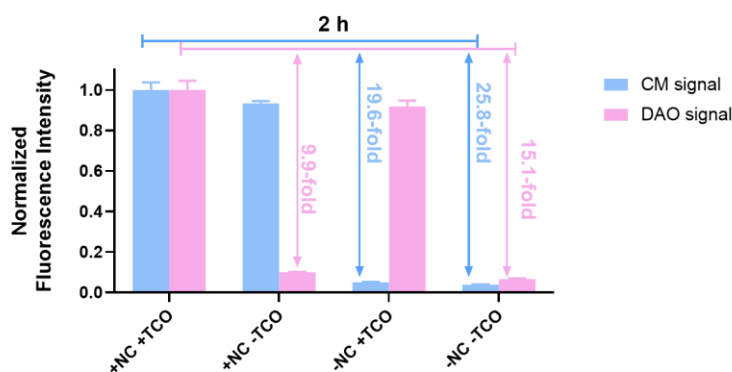


Figure S17. Dual fluorophore release by mutually orthogonal cleavage or individual cleavage. The fluorescence intensity of CM and DAO at 2 h was normalized respectively.

Monitored by the corresponding fluorescence turn-on signal, there was no significant cleavage between **iPrTz-DAO** and **1A-NC**, neither between **1B-CM** and **TCO-OH**, which verified the orthogonality between the two cleavage reactions. When the two reactions were conducted in one pot, the fluorescence signals of two channels rised simultaneously.

12. Mutually orthogonal release of fluorophores involving RNA template

In 10% DMSO/PBS (pH 7.2), reagents involved in two mutually orthogonal cleavage reactions were added as indicated below designed for four groups. The mixture was vortexed and incubated at 37 °C. The fluorescence signal of CM ($\lambda_{\text{ex}} = 373 \text{ nm}$, $\lambda_{\text{em}} = 464 \text{ nm}$, both with bandwidth of 20 nm) and DAO ($\lambda_{\text{ex}} = 620 \text{ nm}$, $\lambda_{\text{em}} = 660 \text{ nm}$, both with bandwidth of 20 nm) was measured in a row at indicated time point by a TECAN Spark multifunctional microplate reader.

Reagent	Conc.	+NC +TCO	+NC -TCO	-NC +TCO	-NC -TCO
r1C	100 nM	+	+	+	+
r1B-CM	100 nM	+	+	+	+
iPrTz-DAO	0.5 μM	+	+	+	+
r1A-NC	100 nM	+	+	-	-
TCO-OH	5.0 μM	+	-	+	-

Attendance reagent (+), or no reagent (-)

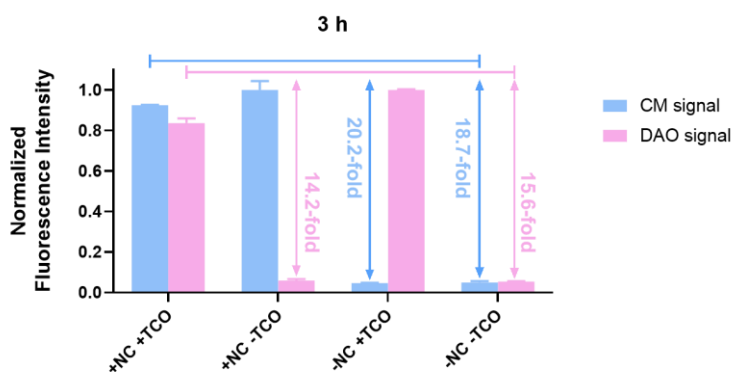


Figure S18. Dual fluorophore release by mutually orthogonal cleavage or individual cleavage. The fluorescence intensity of CM and DAO at 3 h was normalized respectively.

13. Live cell confocal fluorescence imaging

Human Skin Fibroblasts (HSF) and SKOV3 cells were cultured in high-glucose DMEM basic (Gibco) supplemented with 10% fetal bovine serum (Gibco). Cells were maintained in 10-cm culture dishes (NEST) at 37 °C under humidified atmosphere containing 5% CO₂.

For live cell confocal fluorescence imaging, cells were seeded into a 12-well cell culture plate (BEAVER) and allowed to grow until the confluency of 60%-70%. The attached cells were washed twice with Live Cell Imaging Solution (LCIS, Gibco Invitrogen), then incubated with indicated probe solution in LCIS at 37 °C under humidified atmosphere containing 5% CO₂. Imaging was performed on a LSM 880 system (Carl ZEISS) without washing. The excitation light in the confocal mode was provided by a 405 nm (blue channel), 488 nm (green channel), or 633 nm (red channel) laser.

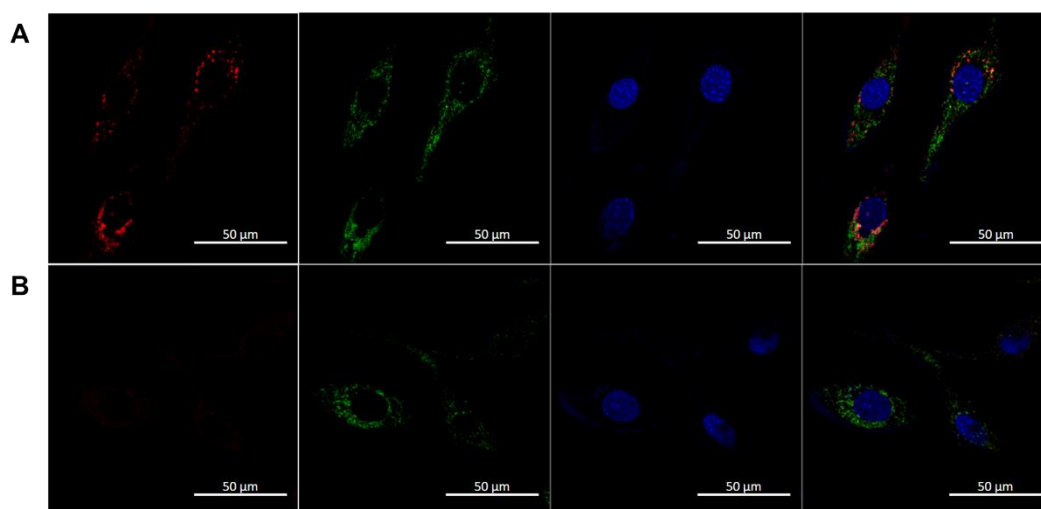


Figure S19. (A) Mitochondria imaging by *t*BuTz-DHX and PhetNC in live SKOV3 cells (red channel). The cells were first incubated with *t*BuTz-DHX (1.5 μM), which was removed after 1 h. The cells were then treated with PhetNC (20 μM), observed by confocal fluorescence imaging after 6 h since the addition of PhetNC. (B) Control imaging without the addition of PhetNC. Green channel, Mito Tracker Green (0.2 μM); blue channel, Hoechst 33342 (10 μM); scale bar, 50 μm.

Red fluorescence staining of mitochondria was clearly imaged in the presence of excess PhetNC (20 μM) without the need of wash, while negligible fluorescence was observed in the absence of PhetNC.

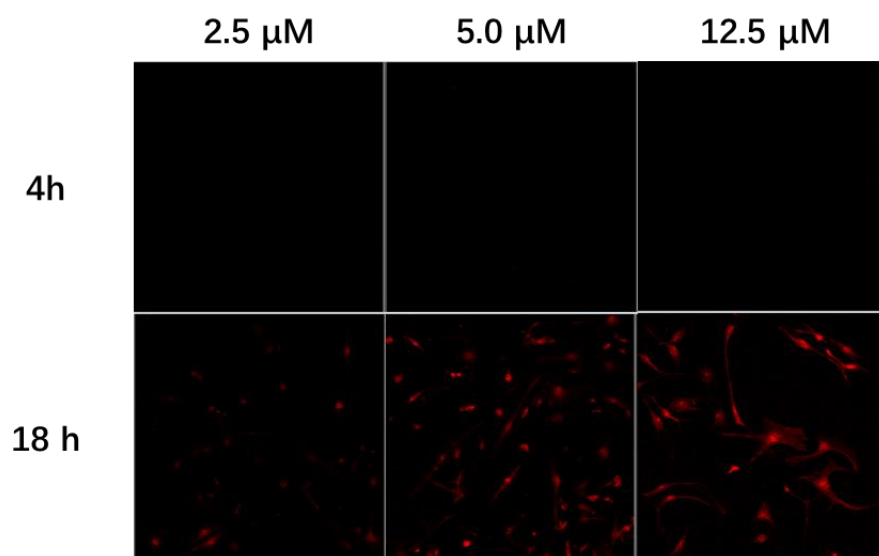


Figure S20. Bioorthogonal cleavage of *iPrTz-DAO* in live HSF cells with different concentrations of **TCO-TPP**. The cells were first incubated with *iPrTz-DAO* (5.0 μM), which was removed after 2 h. The cells were then treated with **TCO-TPP** (2.5 μM , 5.0 μM , or 12.5 μM), observed by confocal fluorescence imaging at indicated time since the addition of **TCO-TPP**.

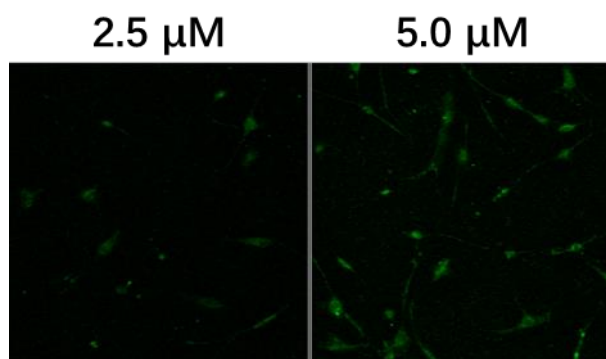
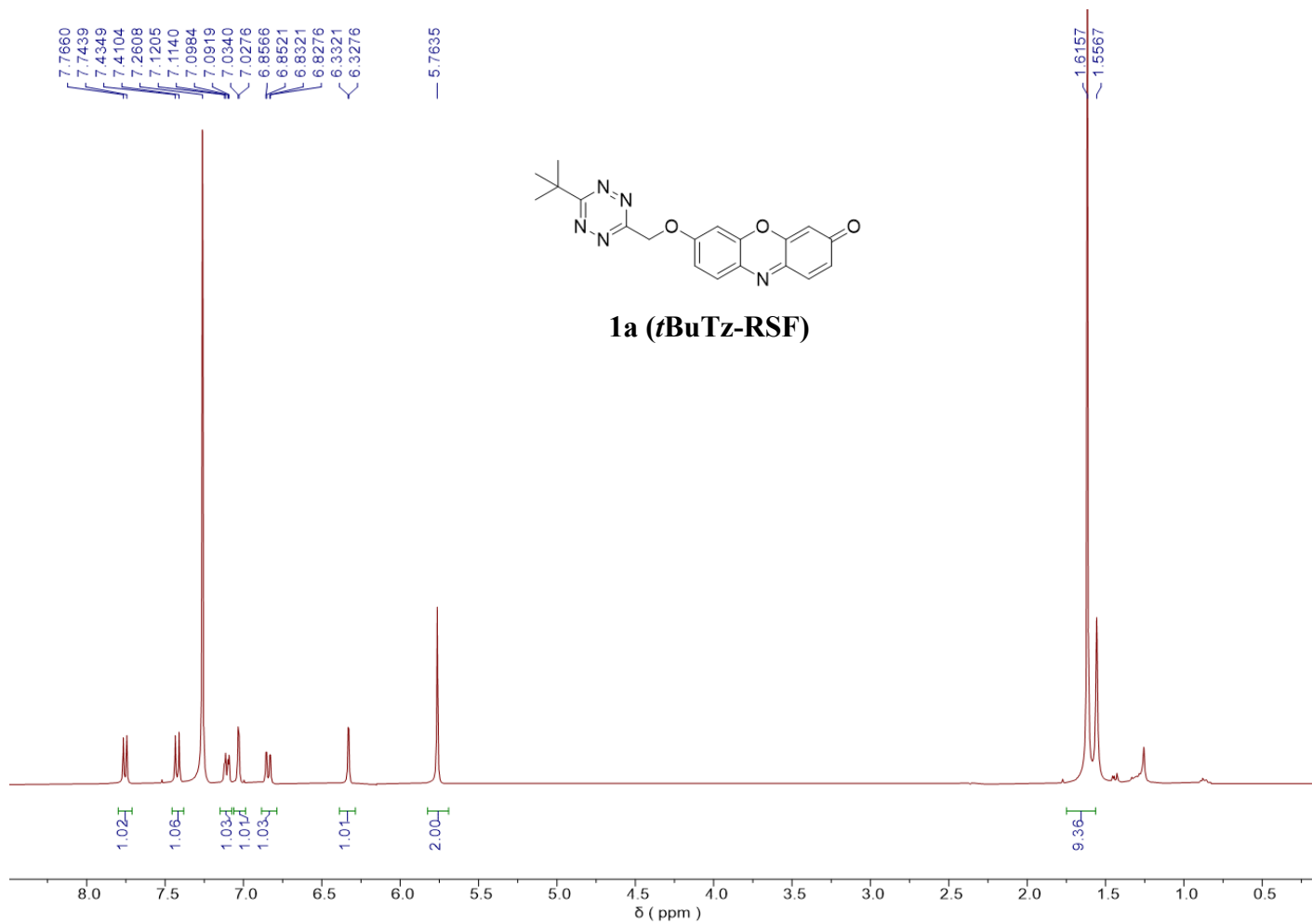
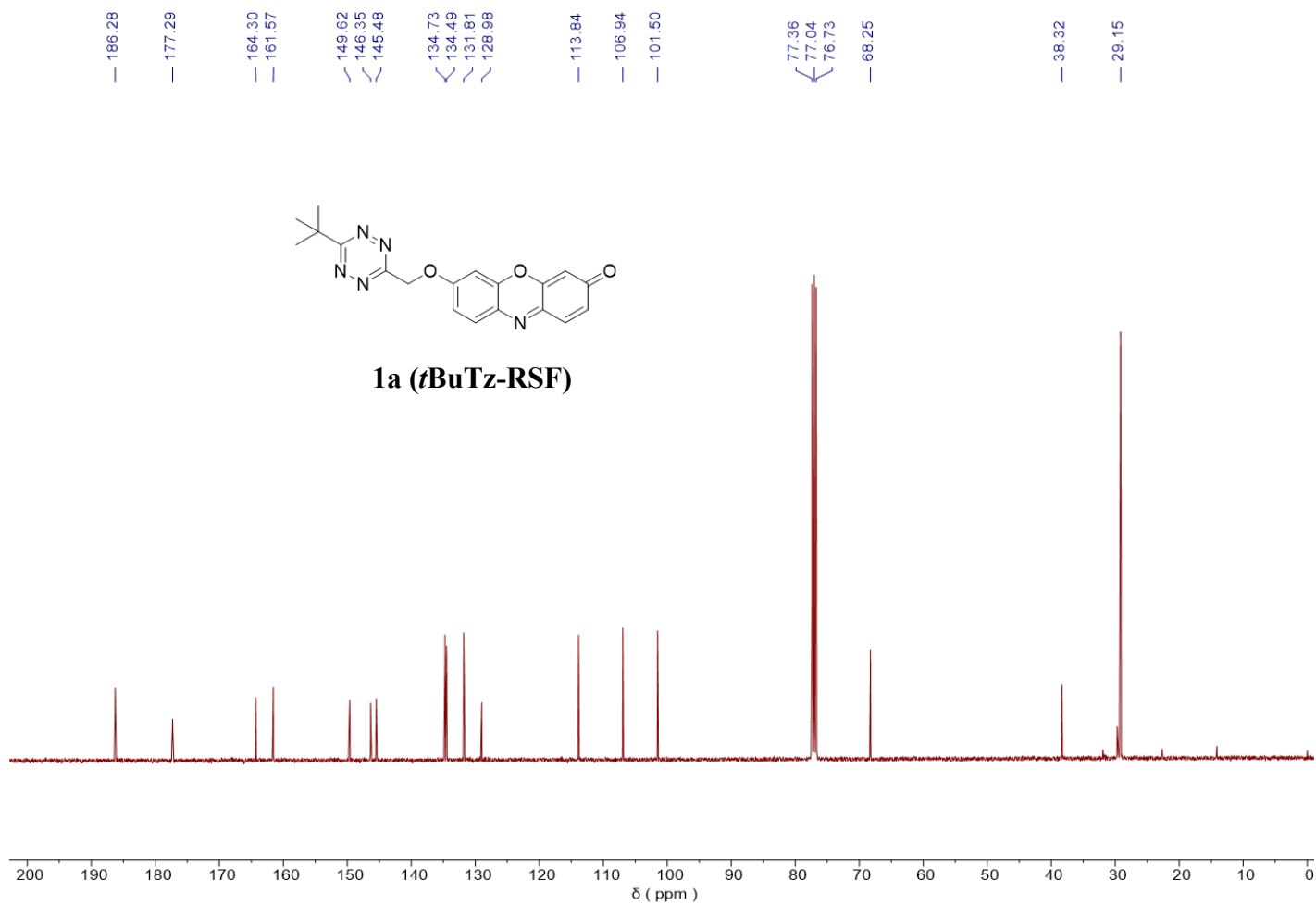
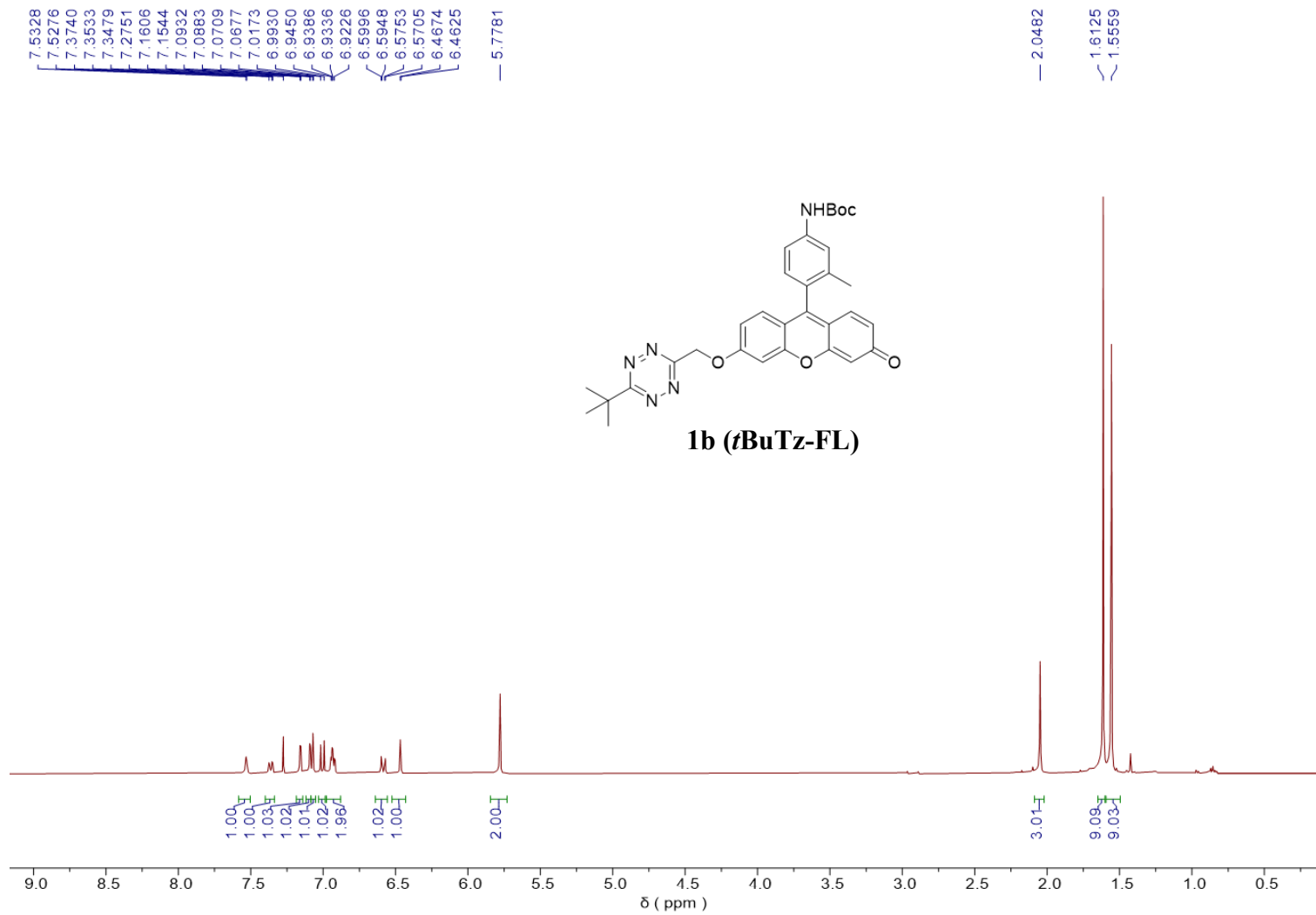


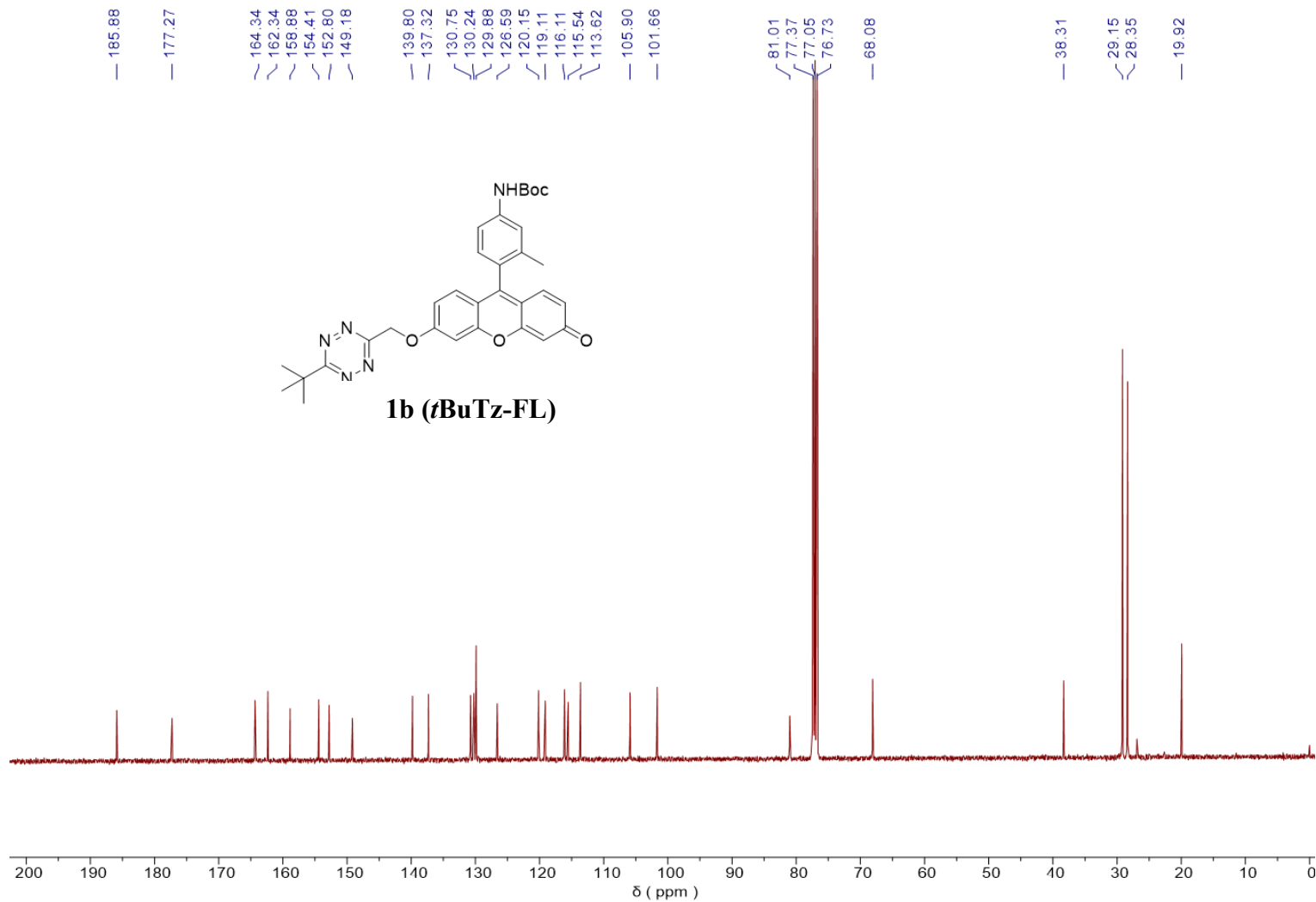
Figure S21. Bioorthogonal cleavage of *tBuTz-FL* in live HSF cells with different concentrations of **PhetNC**. The cells were first incubated with *tBuTz-FL* (1.0 μM), which was removed after 2 h. The cells were then treated with **PhetNC** (2.5 μM or 5.0 μM), observed by confocal fluorescence imaging after 15 h since the addition of **PhetNC**.

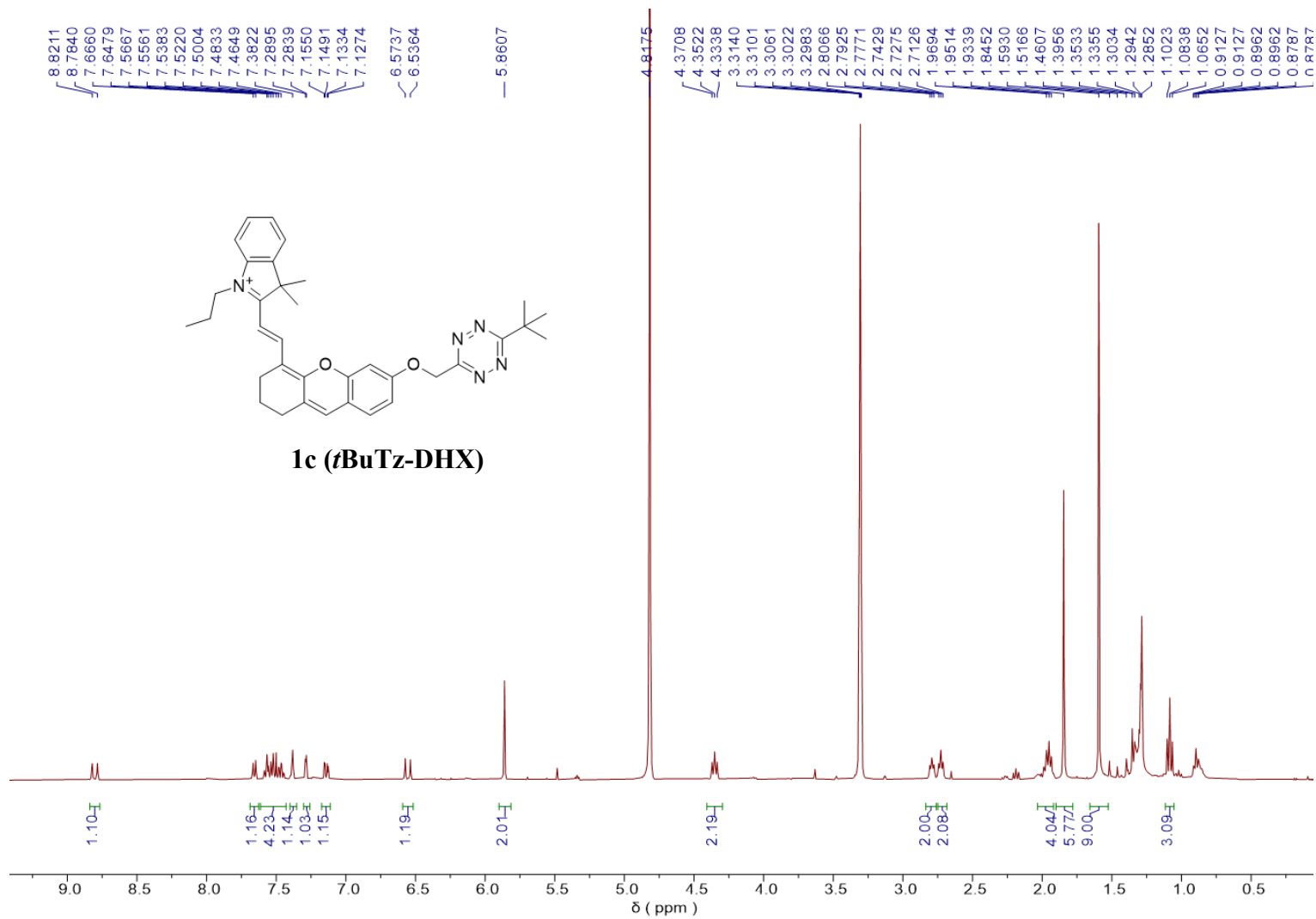
14. Spectra ¹H and ¹³C NMR

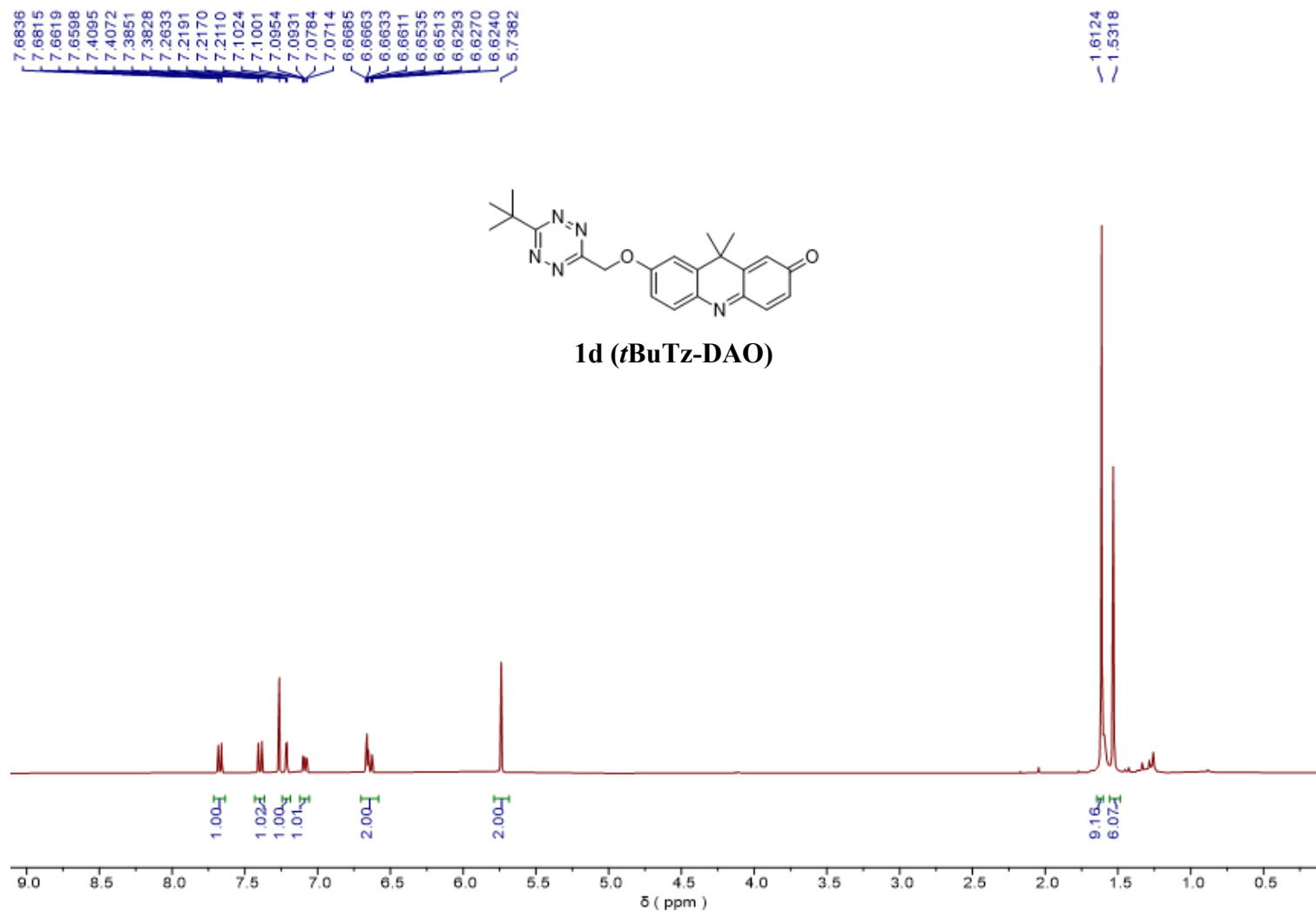


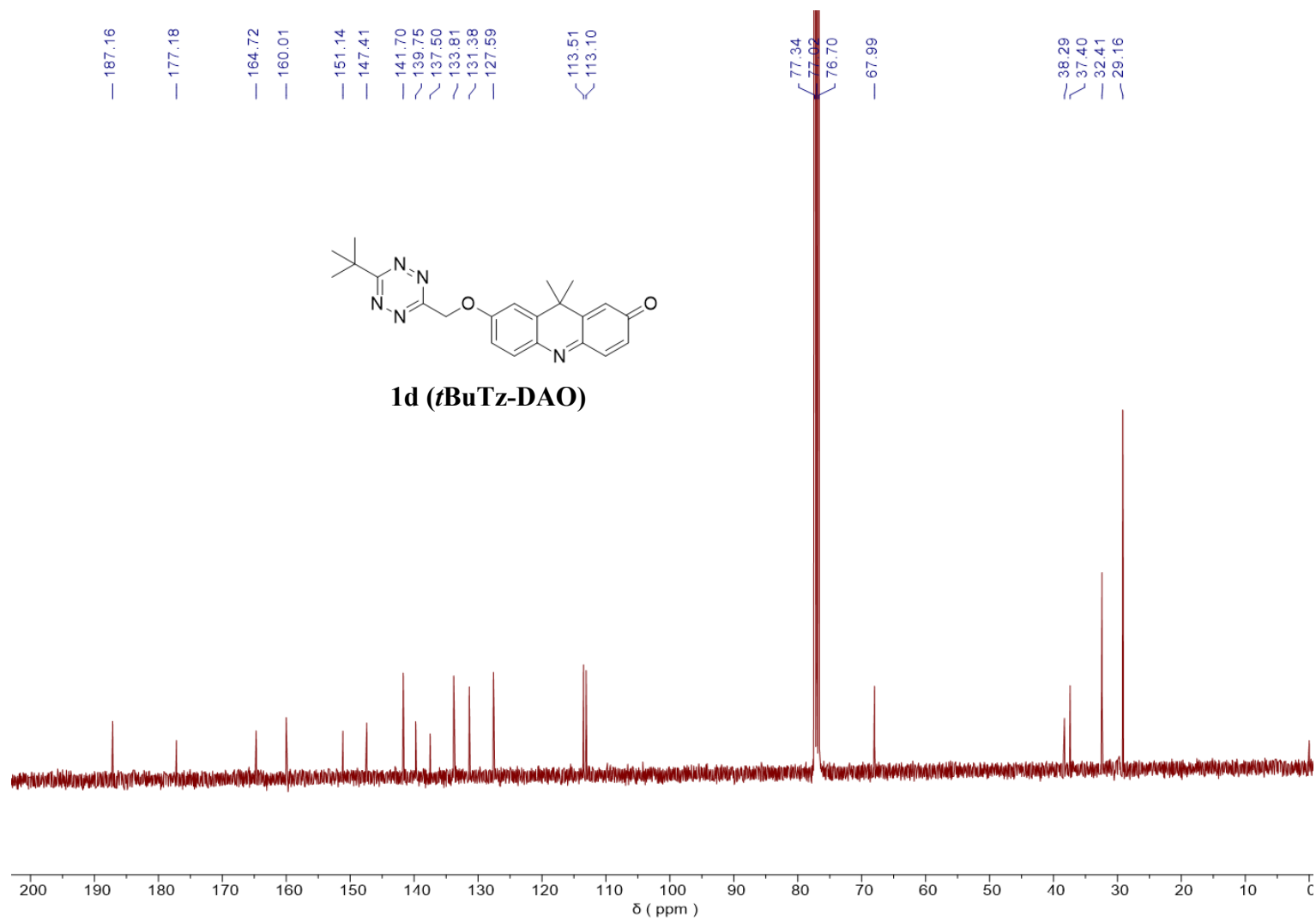


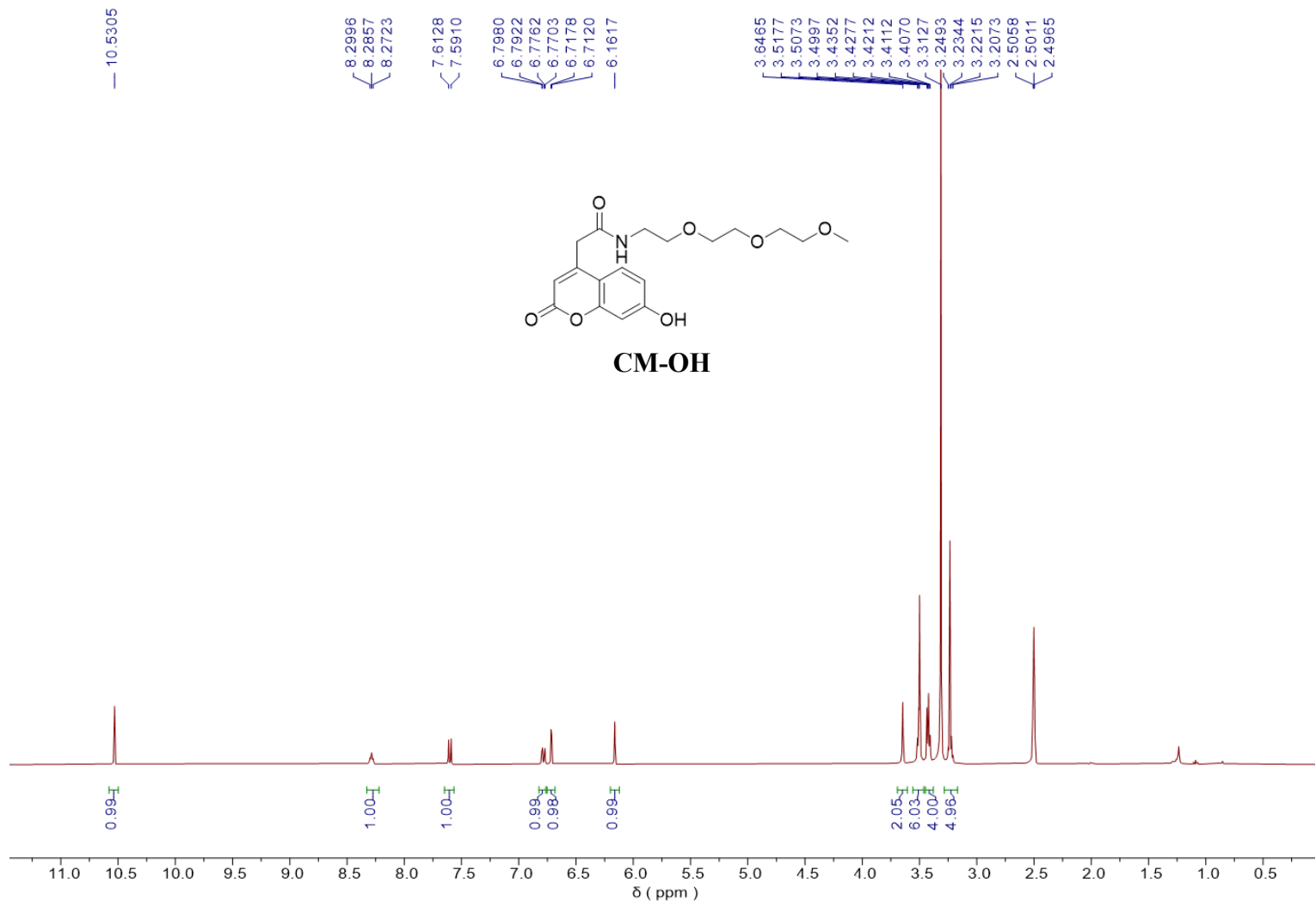


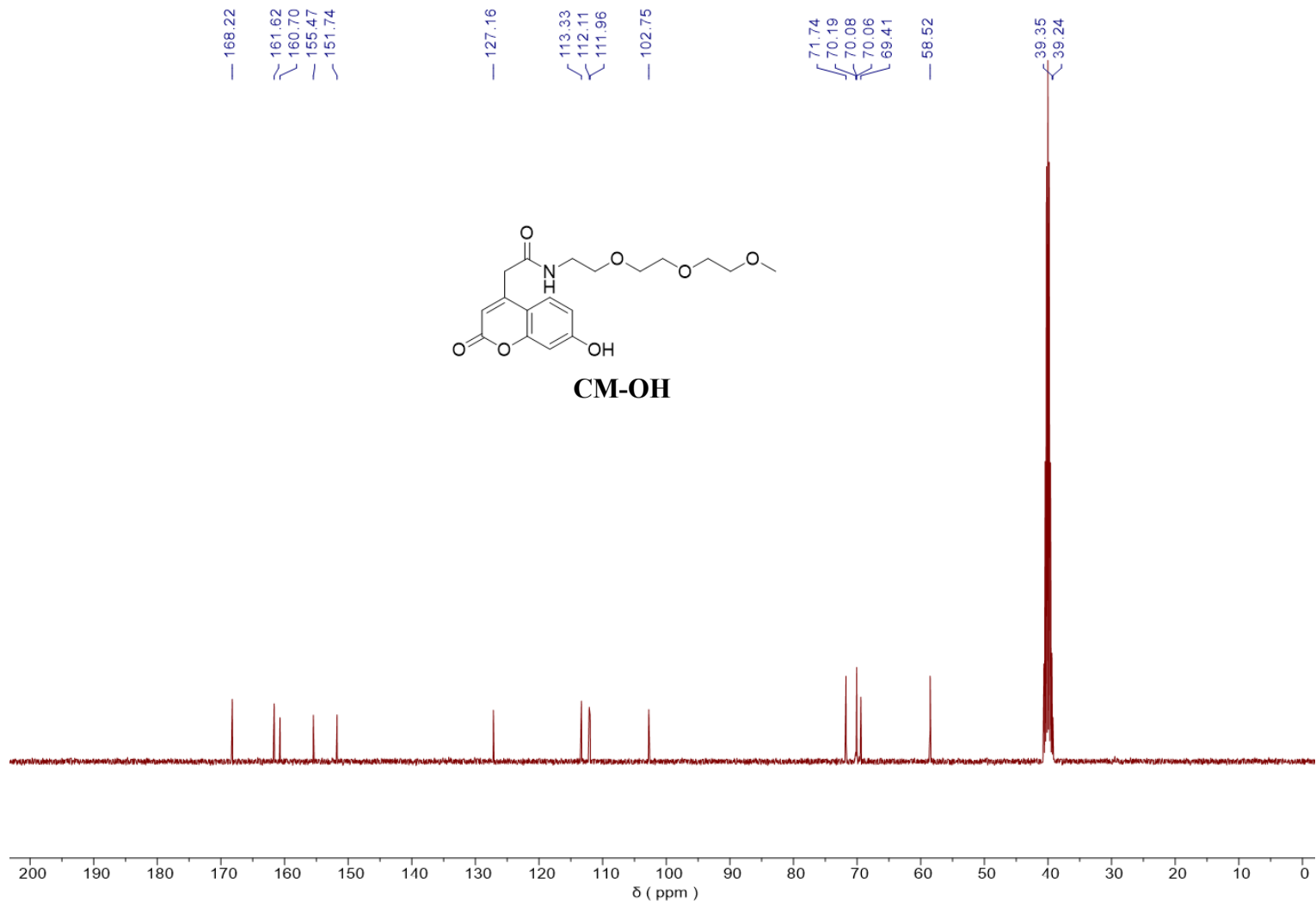


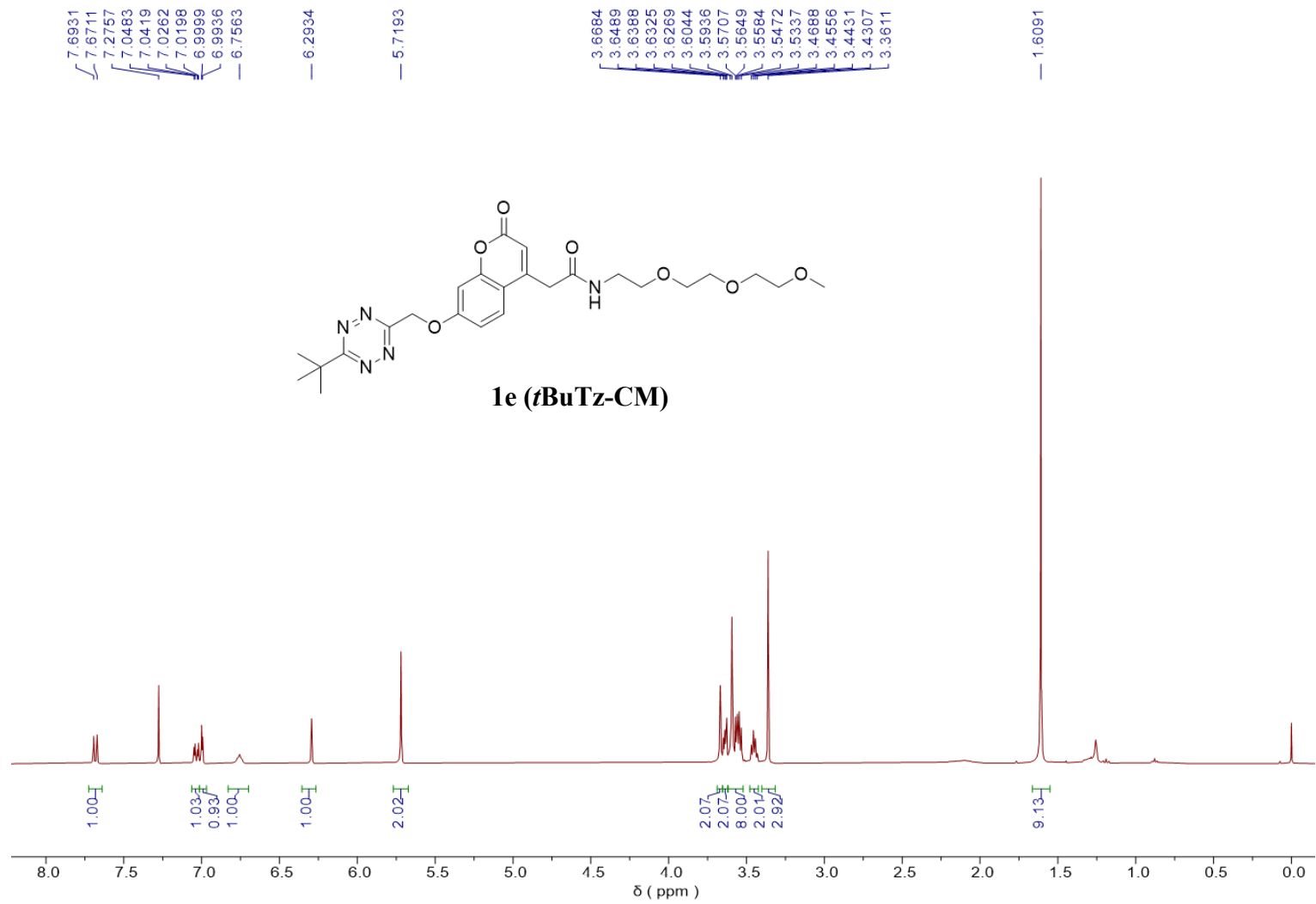


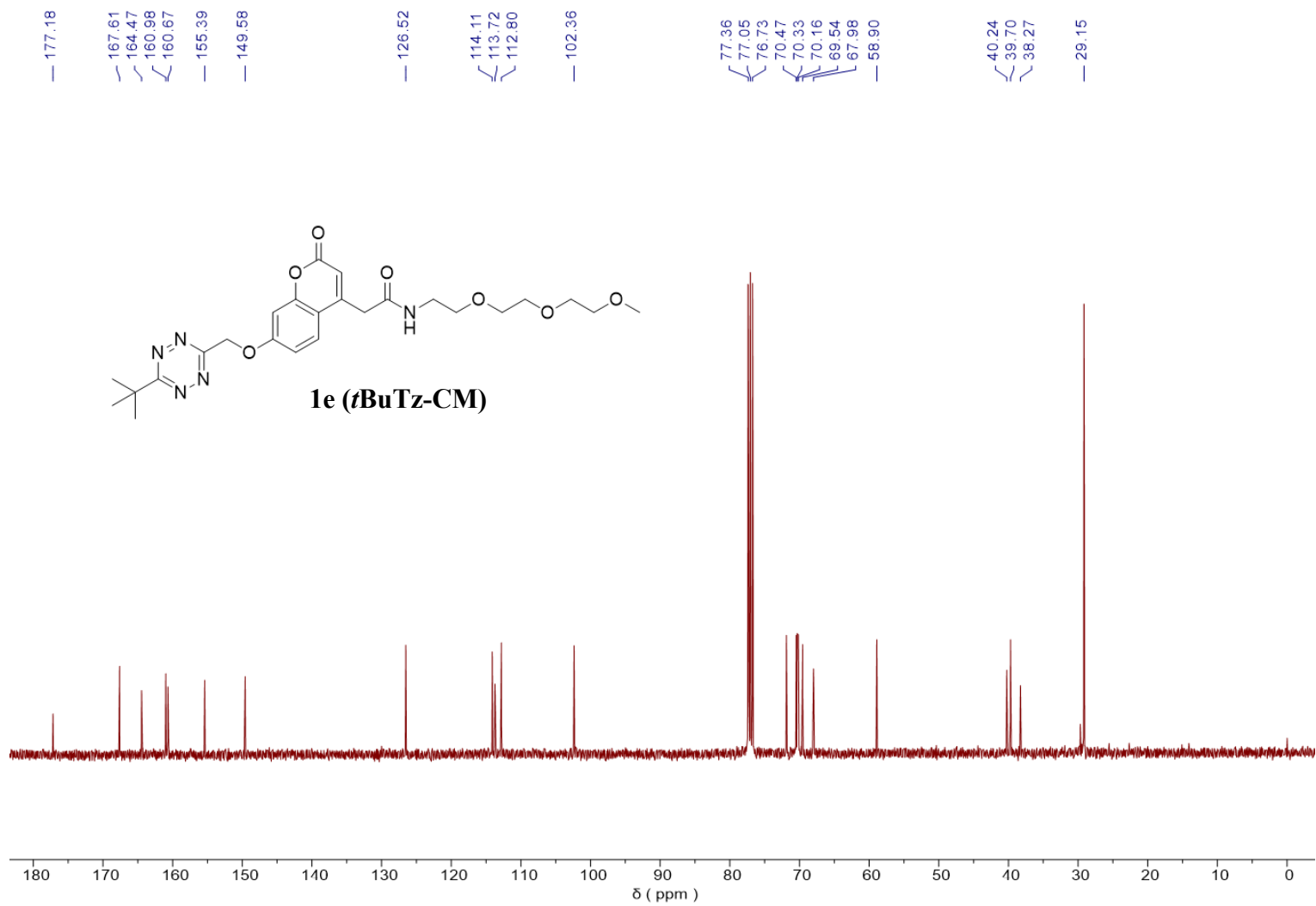


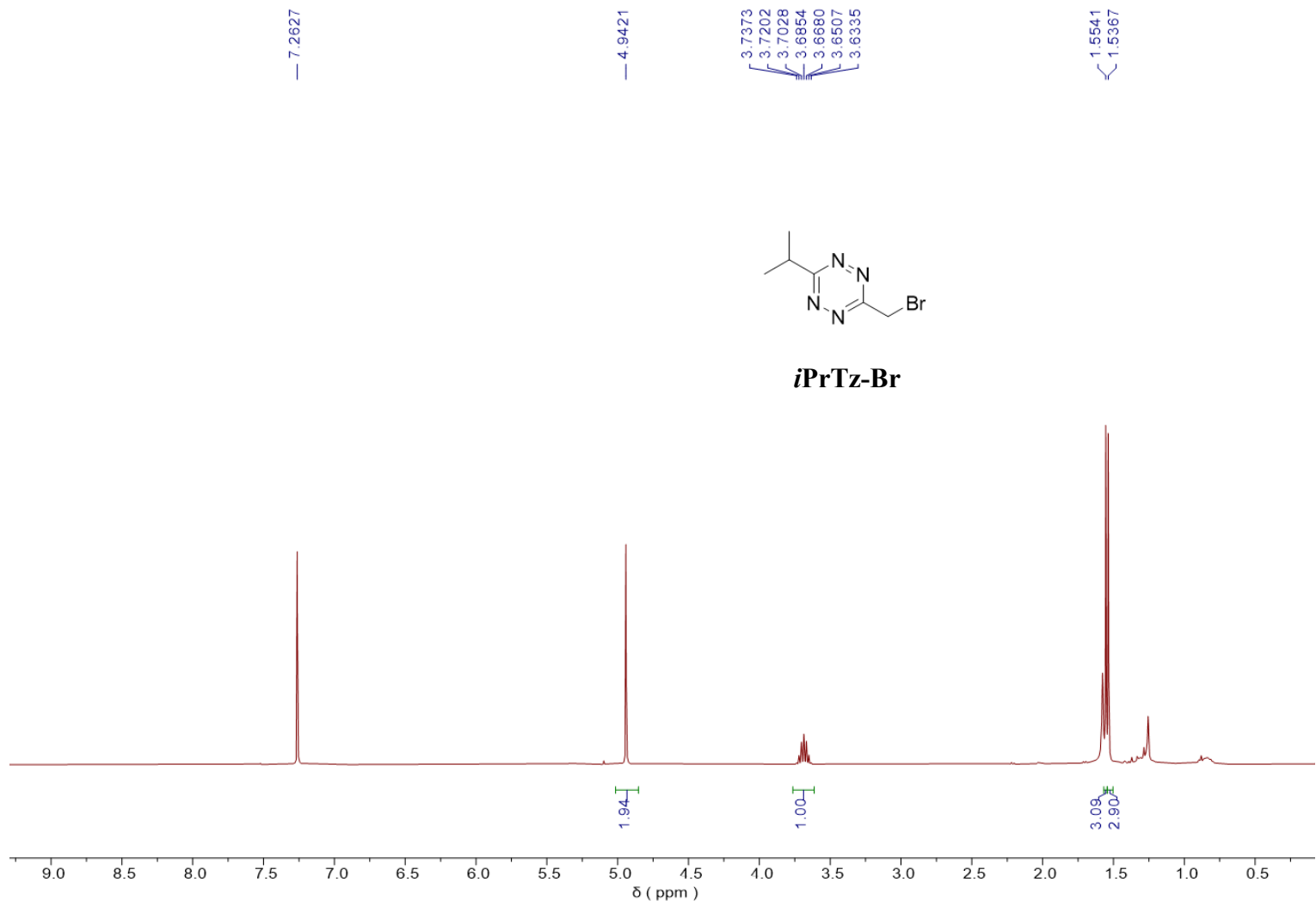


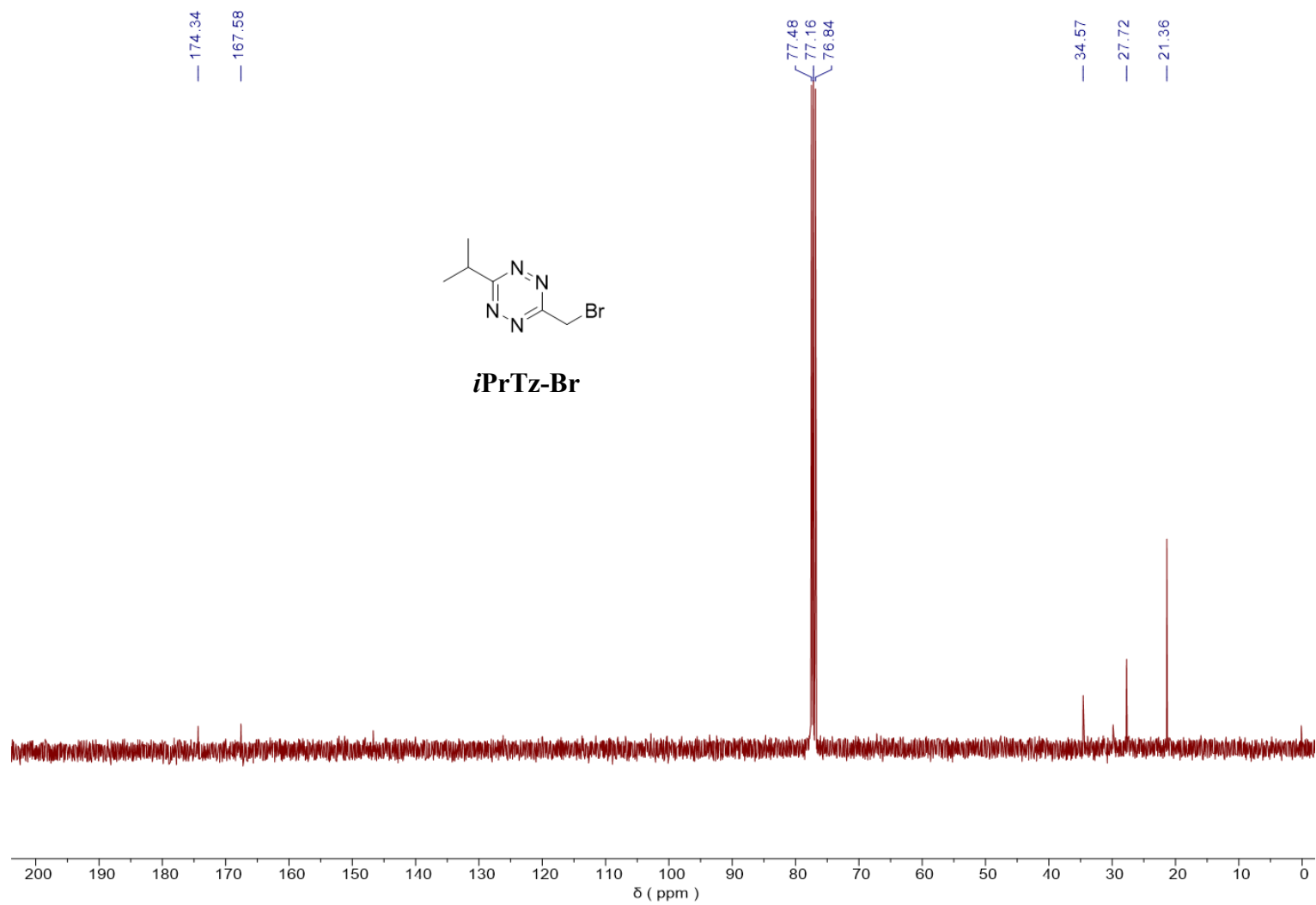


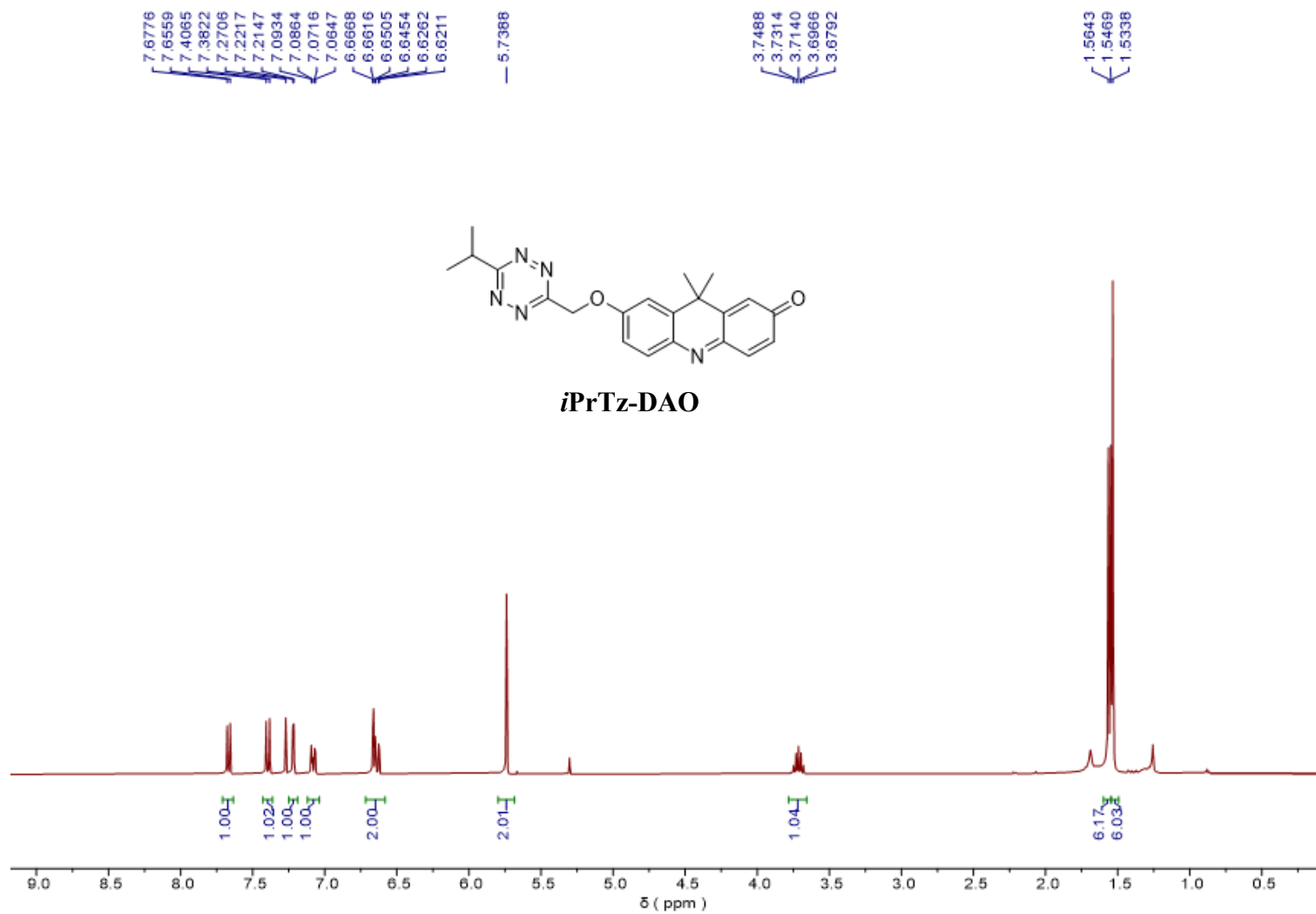


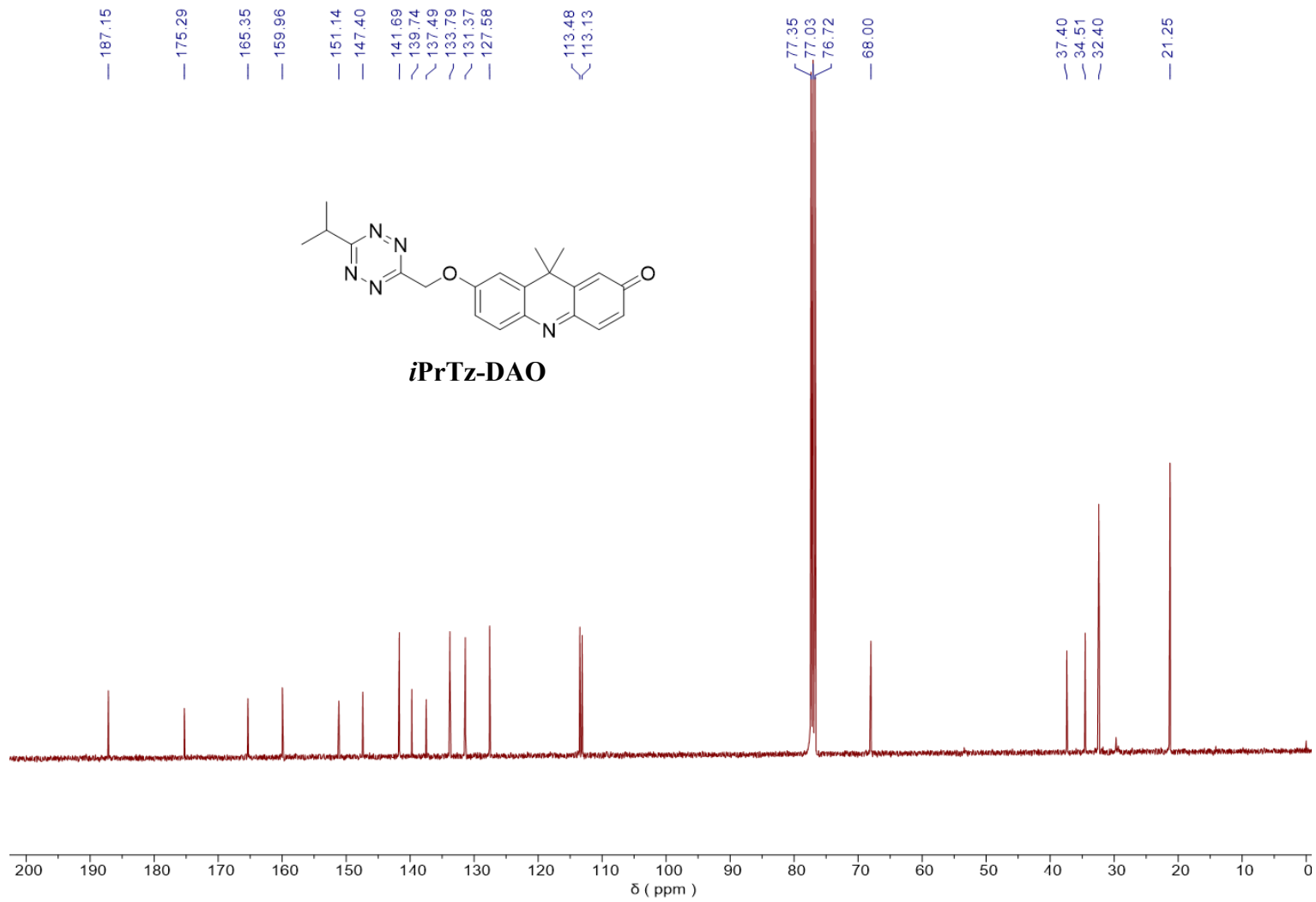


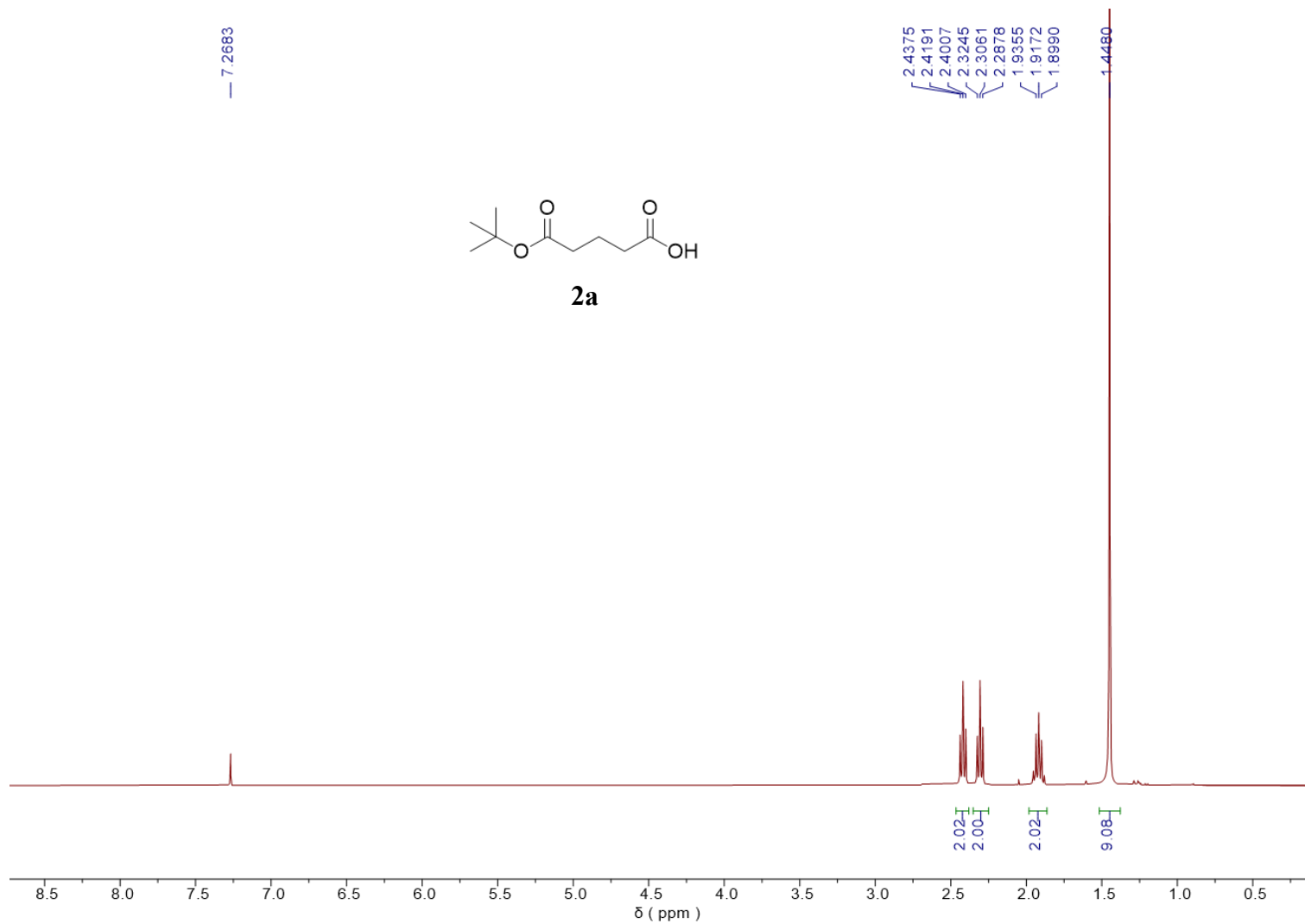


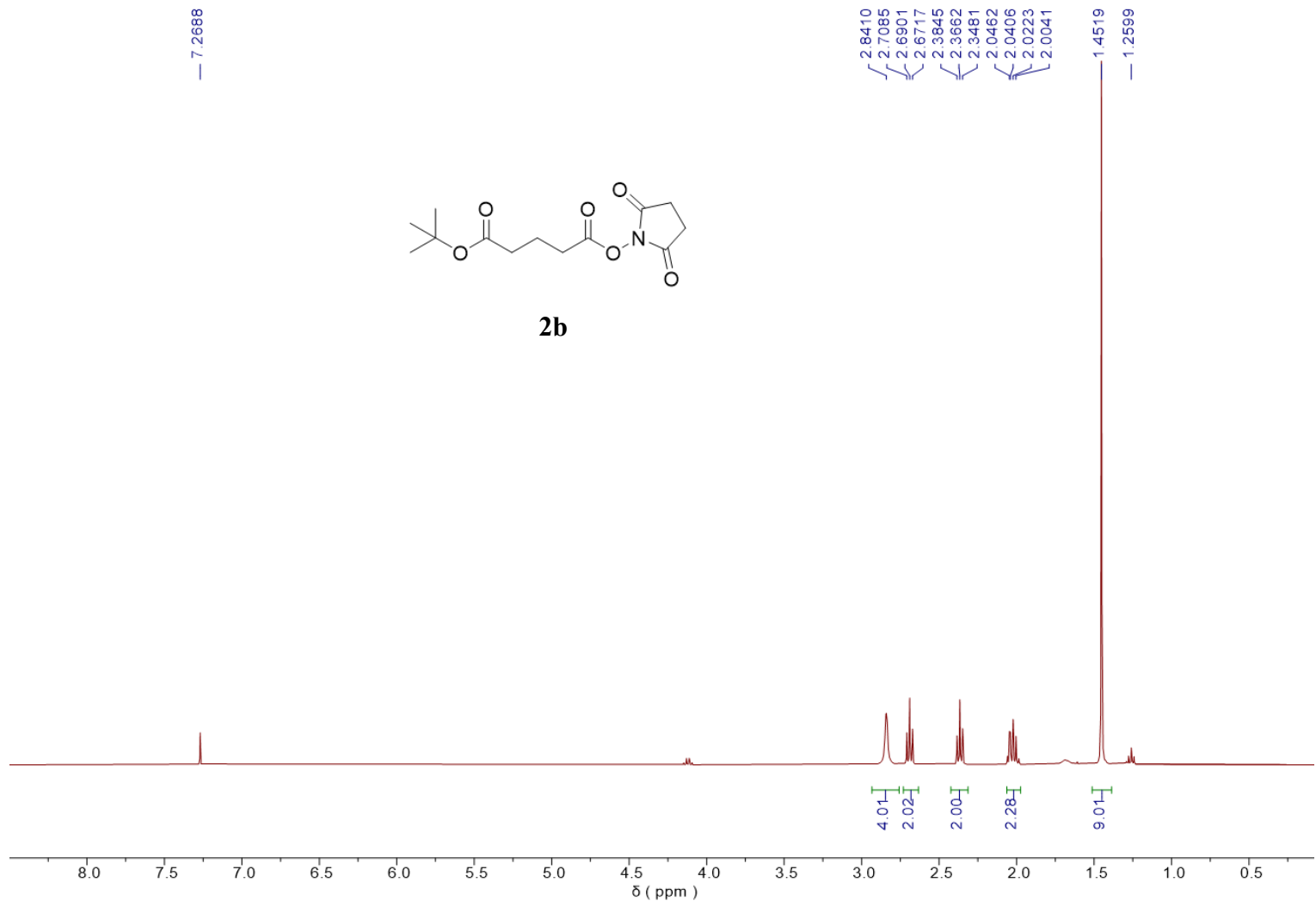


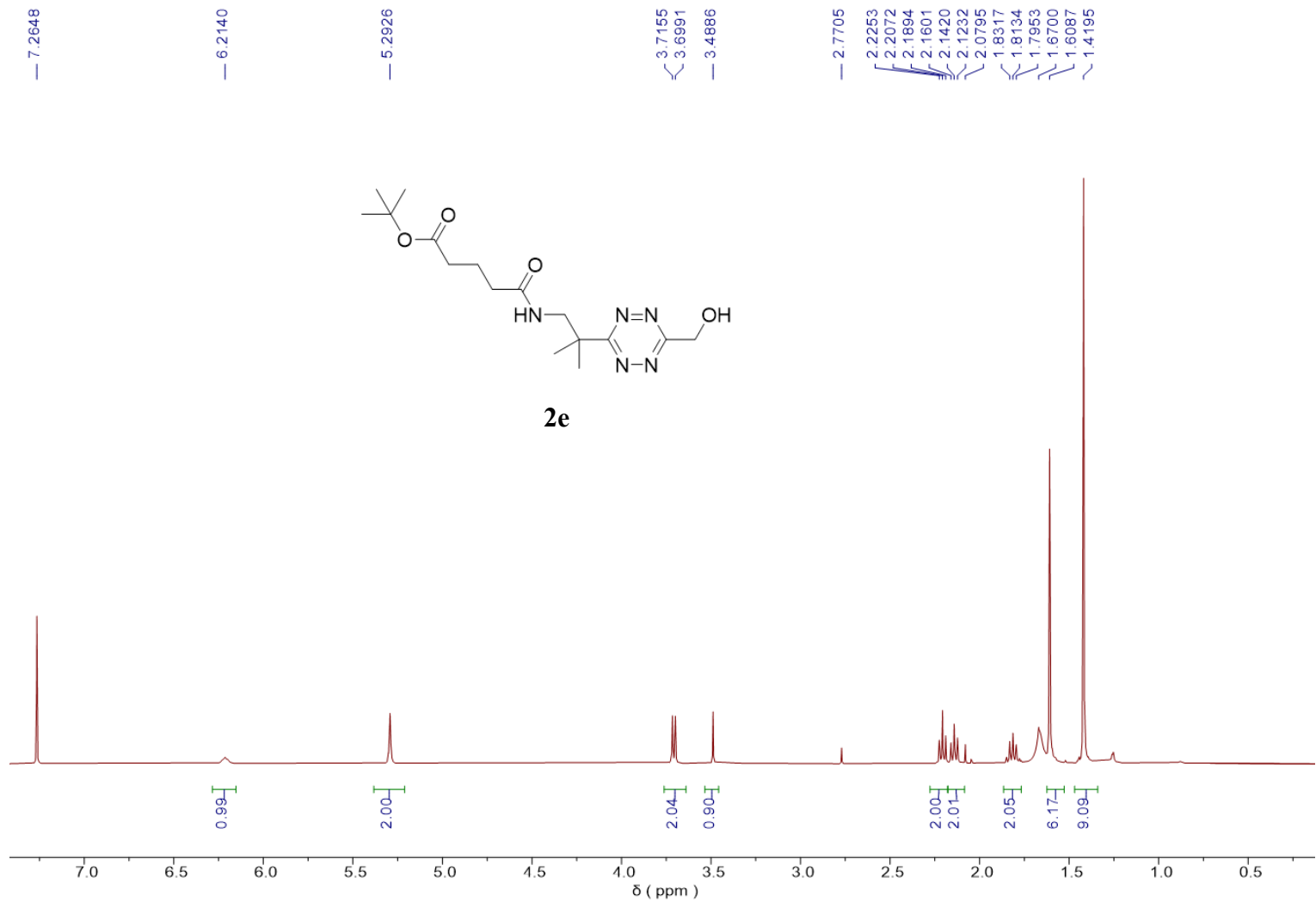


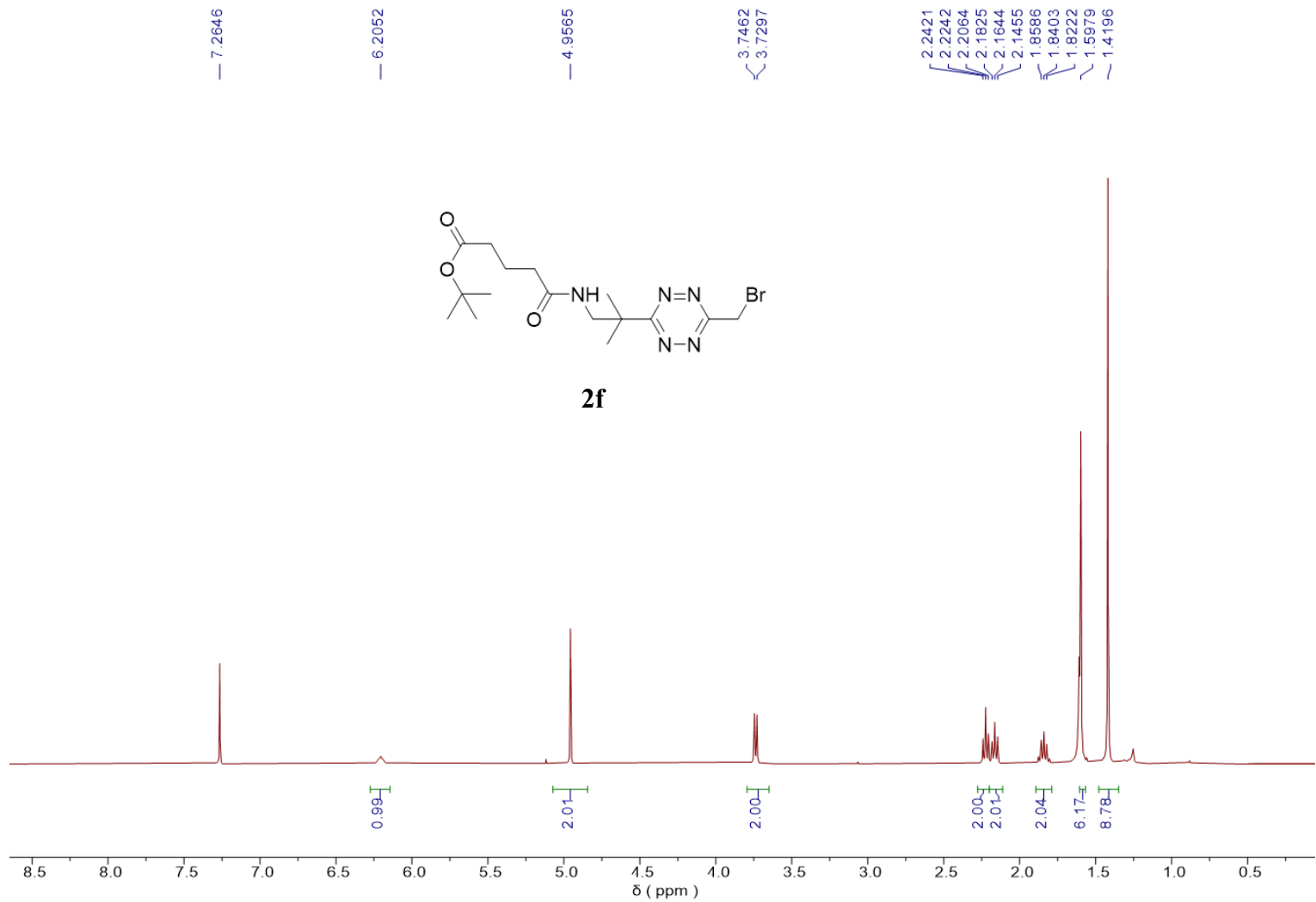


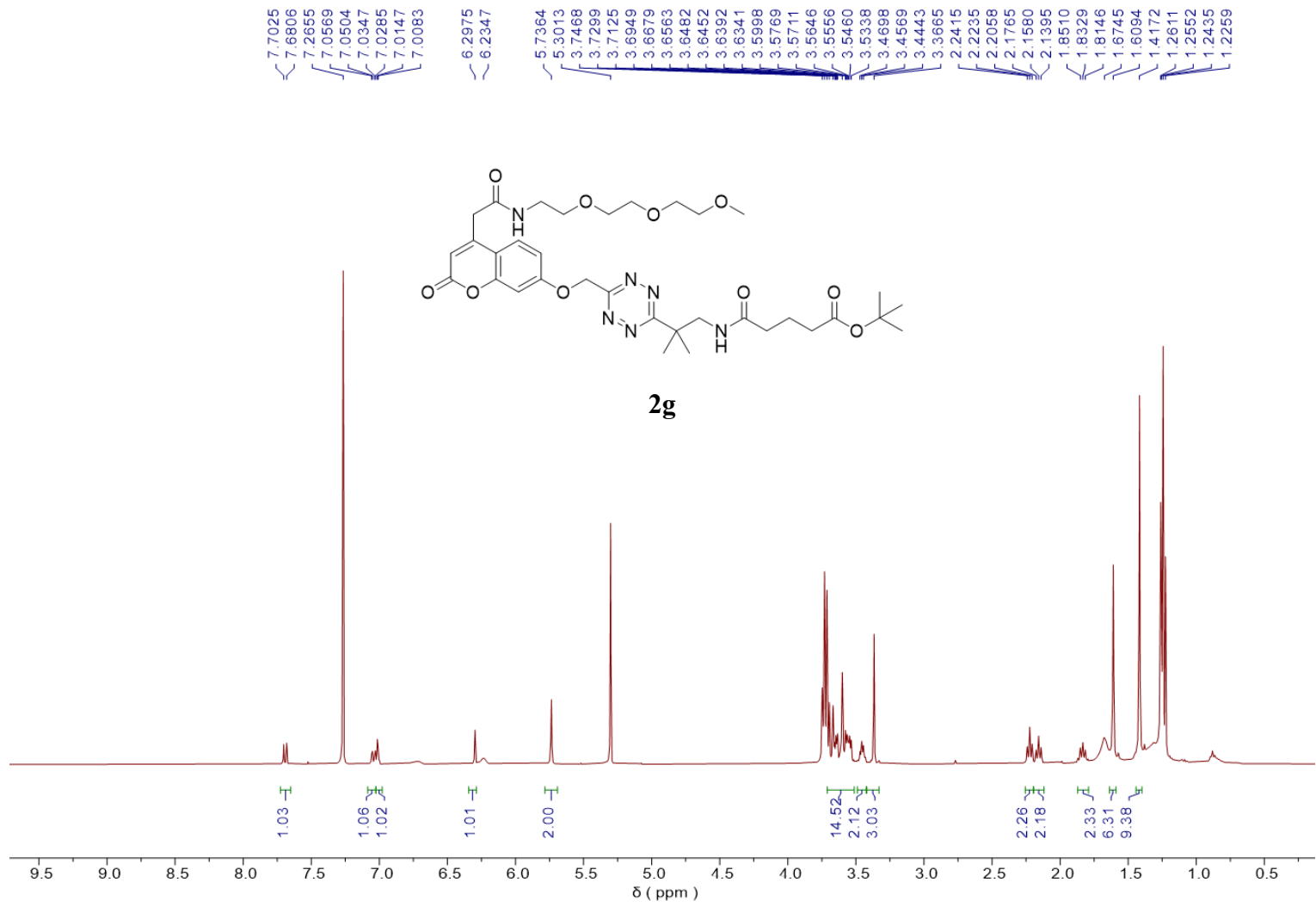


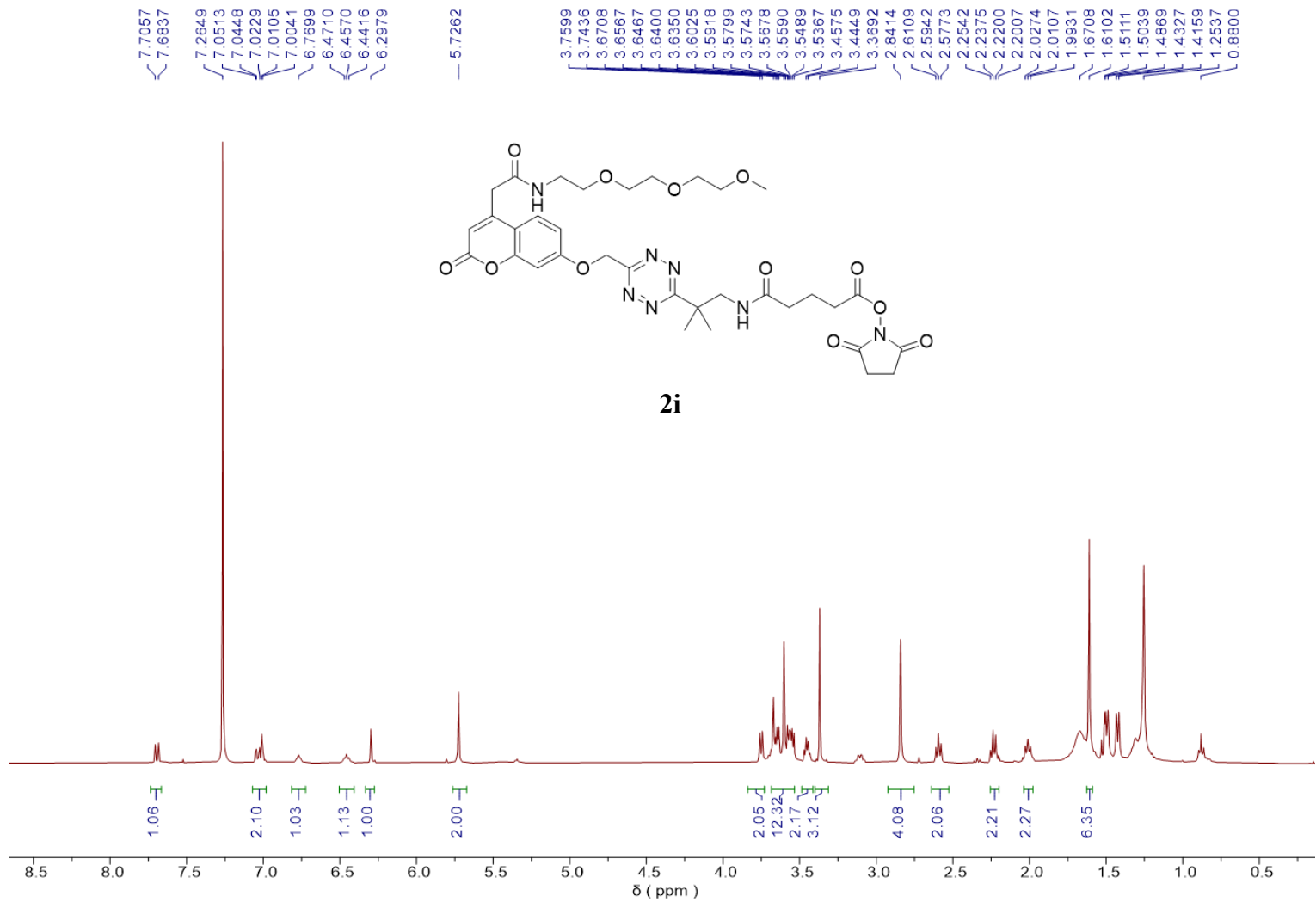


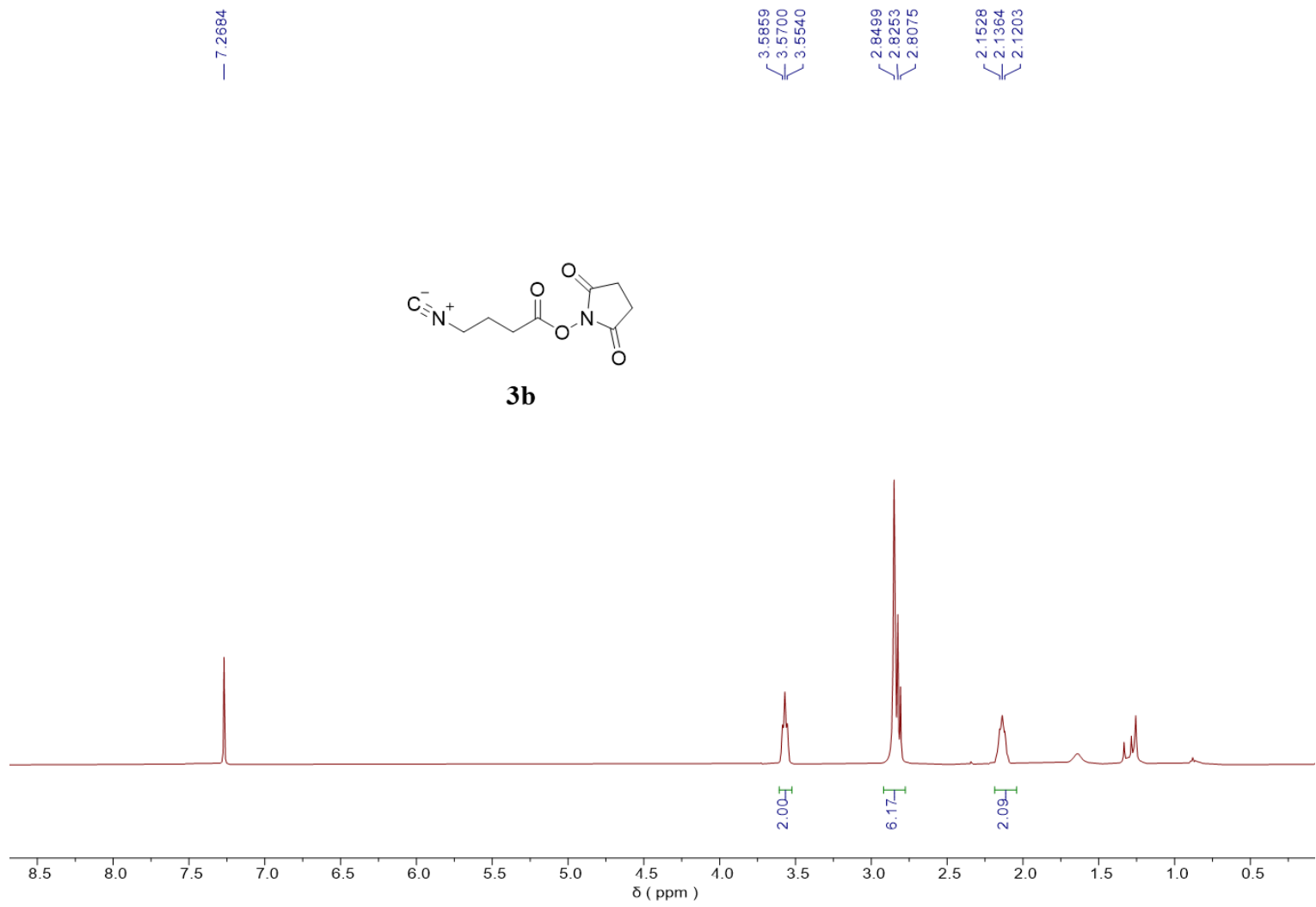


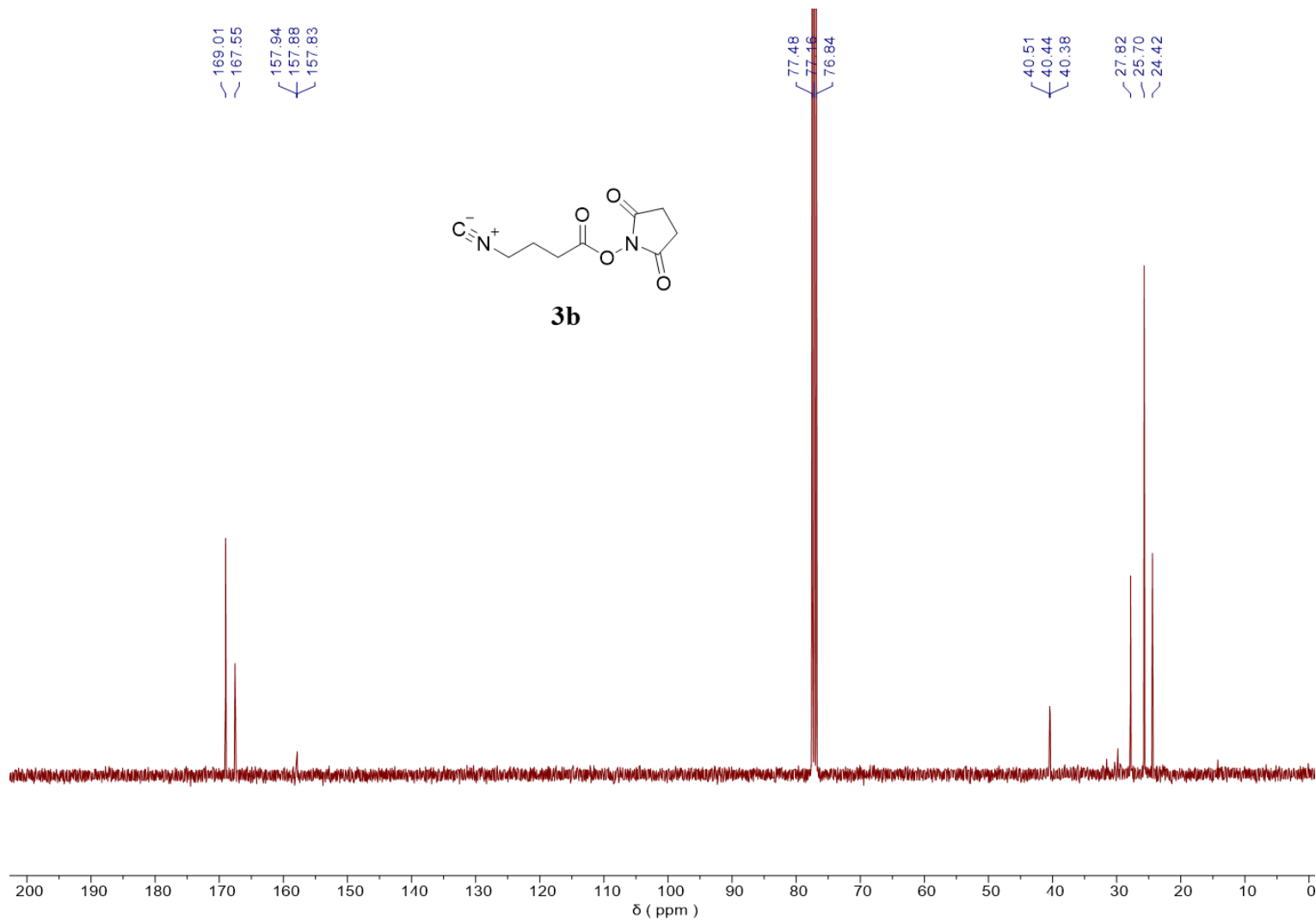






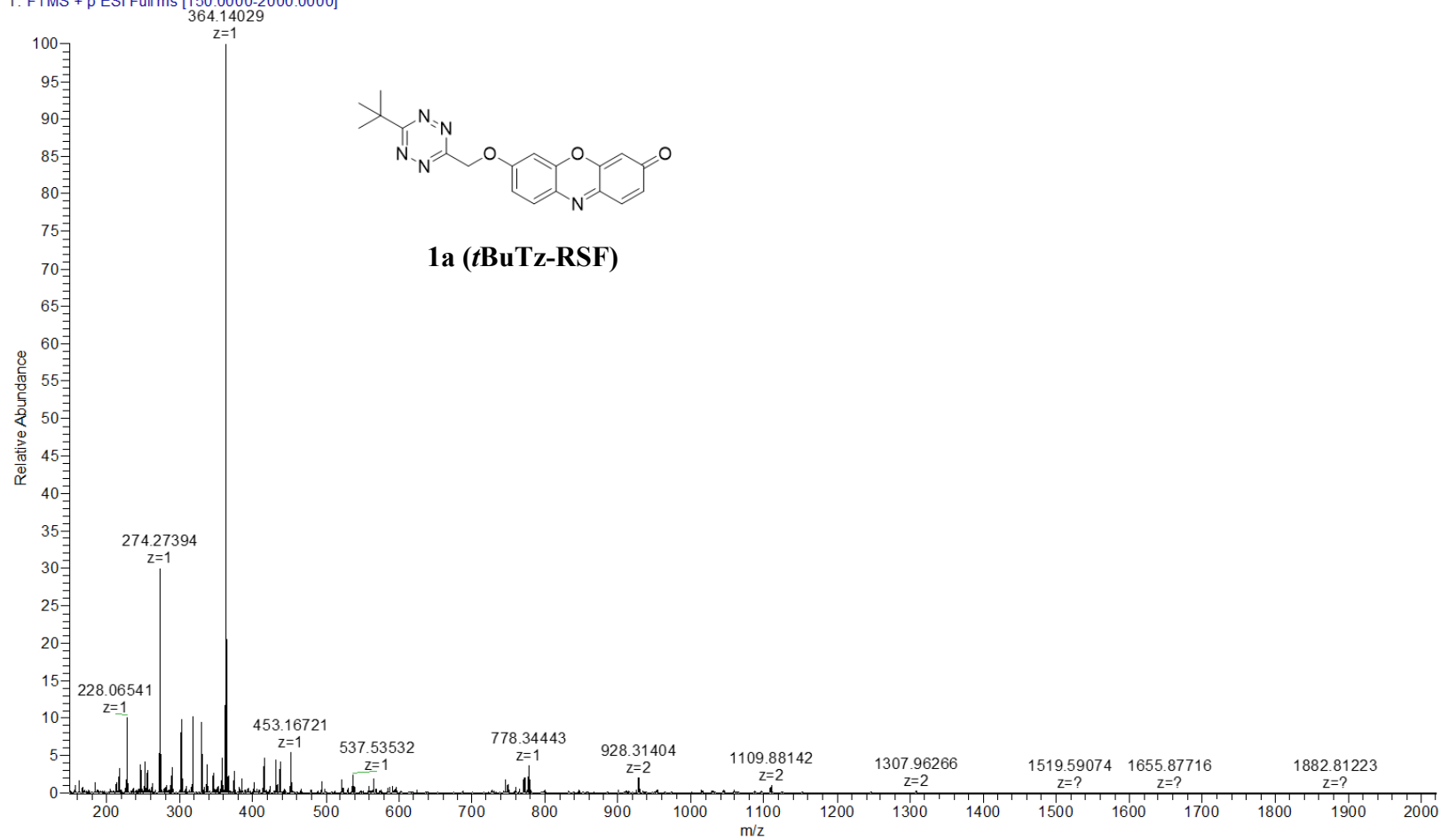






HRMS

2021010308-1 #1-15 RT: 0.00-0.07 AV: 15 NL: 2.00E8
T: FTMS + p ESI Full ms [150.0000-2000.0000]



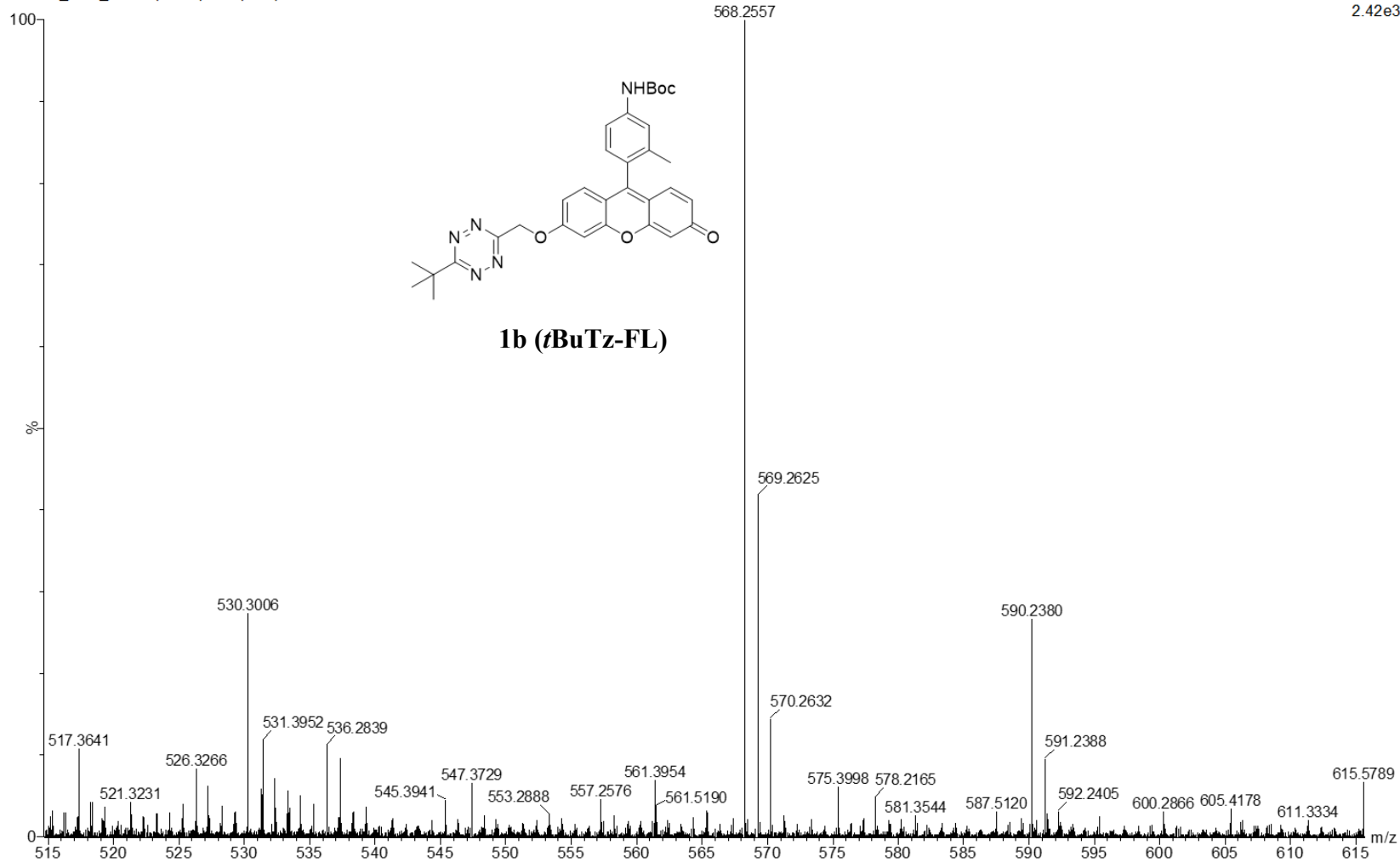
16:22:50

210408_ZXY_02 17 (0.291) Cm (3:24)

08-Apr-2021

TOF MS ES+

2.42e3



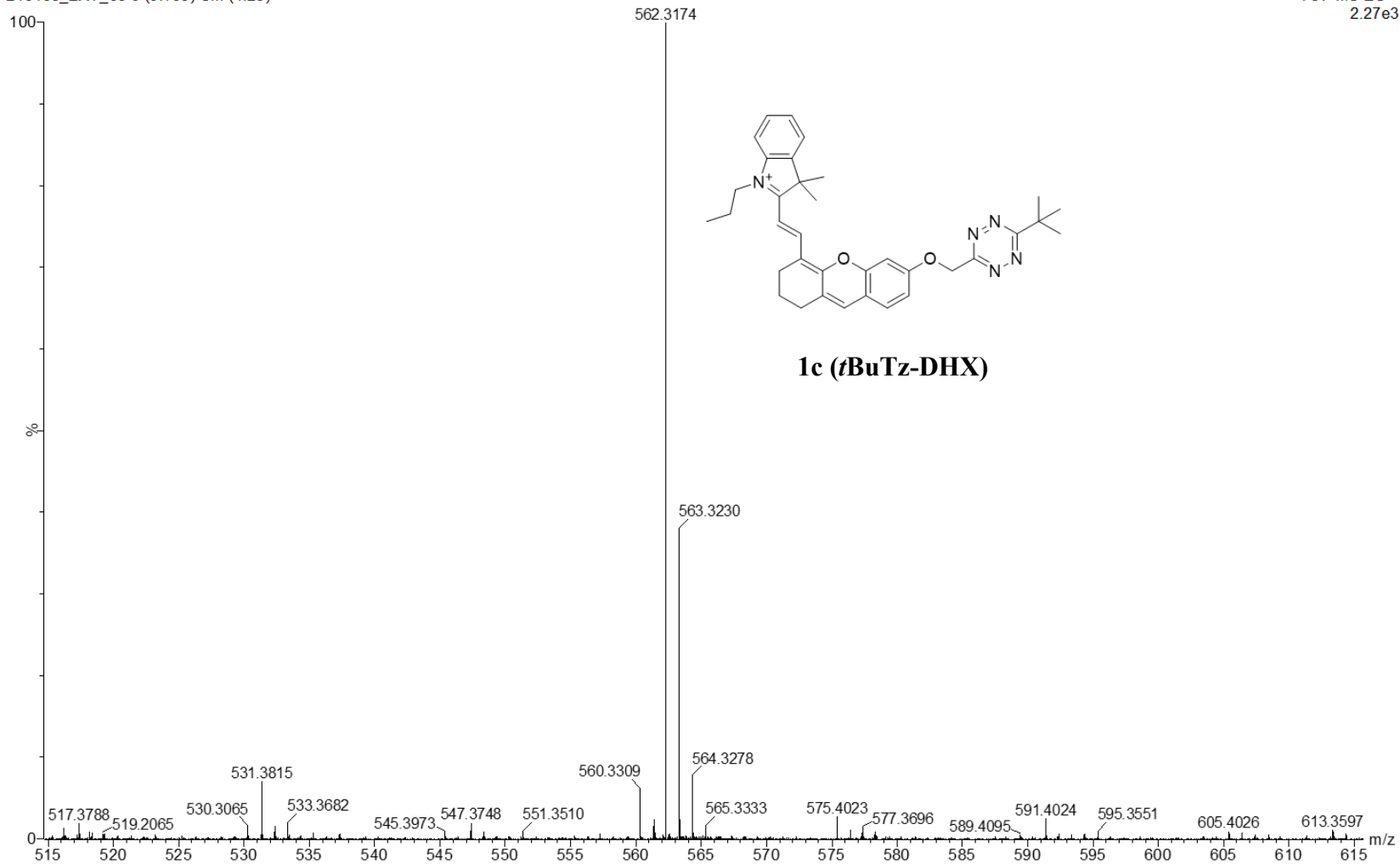
16:24:30

210408_ZXY_03 6 (0.103) Cm (4:23)

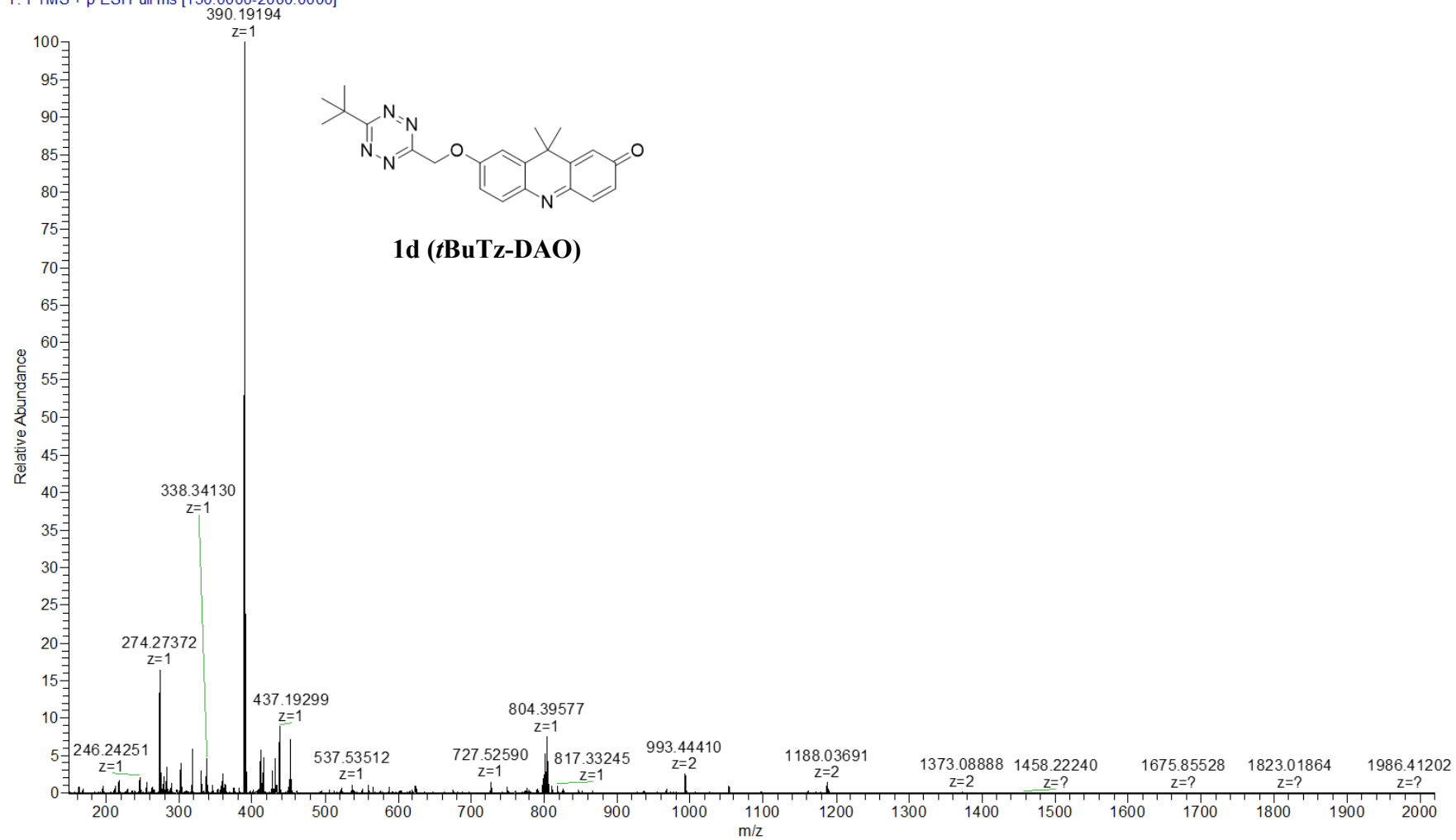
08-Apr-2021

TOF MS ES+

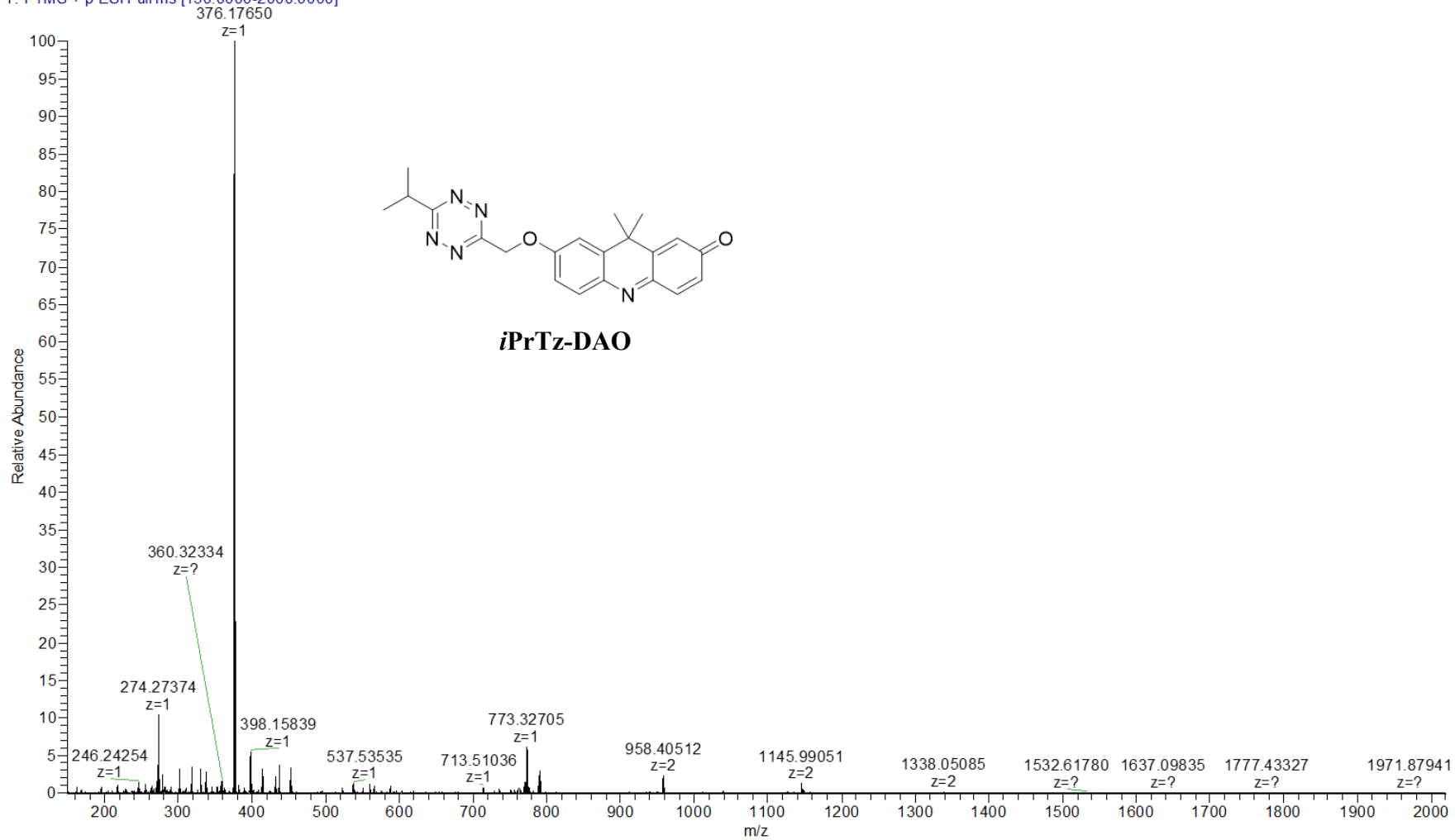
2.27e3



2021010308-2 #1-15 RT: 0.00-0.07 AV: 15 NL: 5.74E8
T: FTMS + p ESI Full ms [150.0000-2000.0000]



2021010308-3 #1-15 RT: 0.00-0.07 AV: 15 NL: 6.48E8
T: FTMS + p ESI Full ms [150.0000-2000.0000]



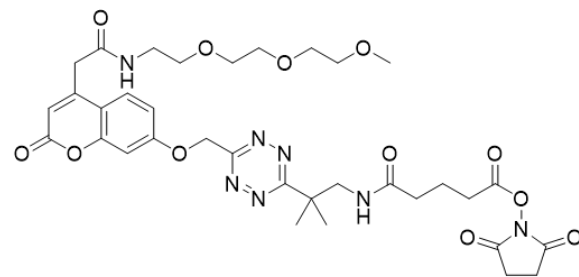
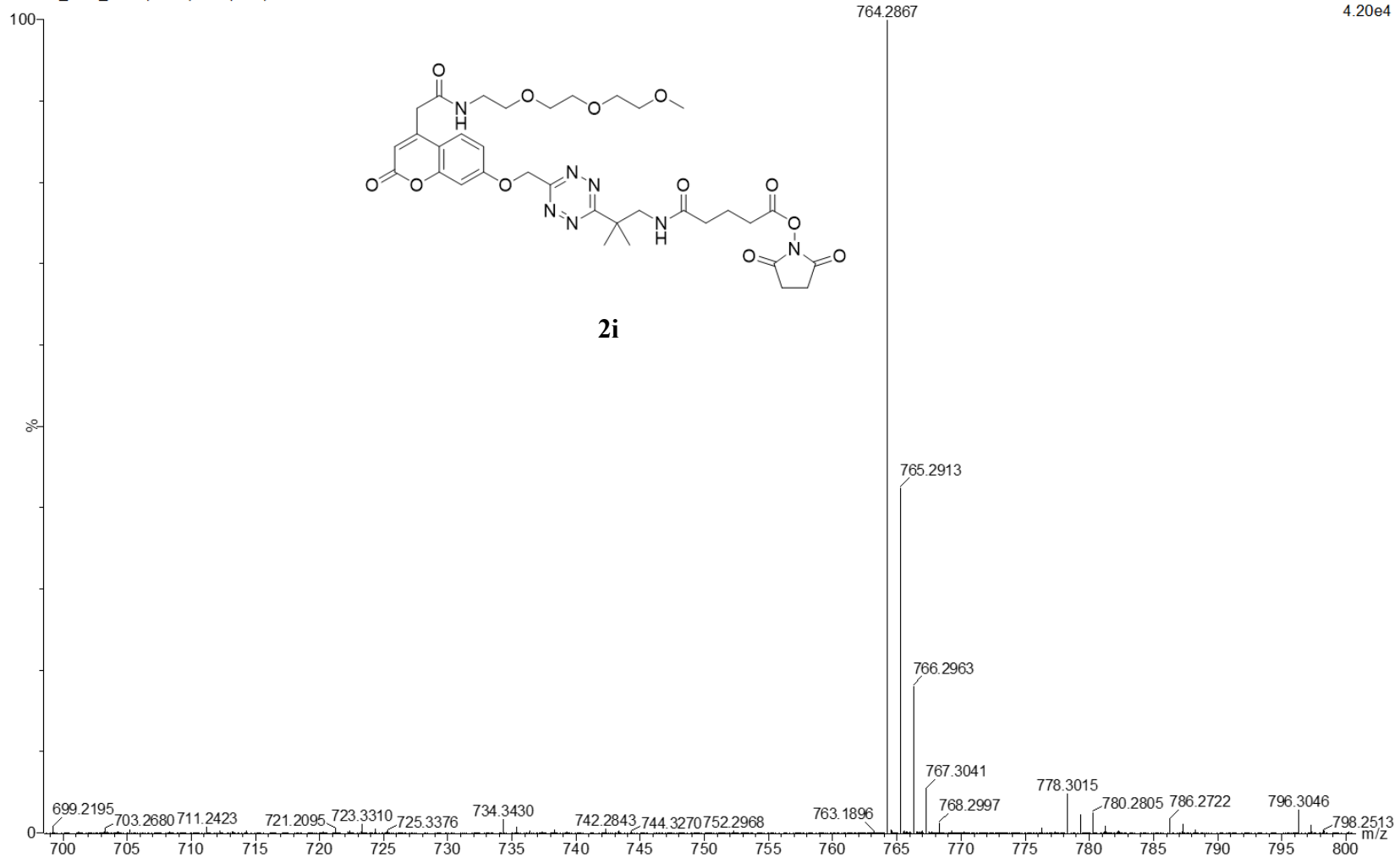
18:00:13

210415_ZXY_12 3 (0.051) Cm (3:23)

15-Apr-2021

TOF MS ES+

4.20e4



2i